IEEE Access
Multidisciplinary | Rapid Review | Open Access Journal

Received May 15, 2021, accepted June 18, 2021, date of publication June 28, 2021, date of current version July 14, 2021.

Digital Object Identifier 10.1109/ACCESS.2021.3092882

Optimizing Energy Harvesting Decode-and-Forward Relays With Decoding Energy Costs and Energy Storage

YANXIN YAO[1], (Member, IEEE), ZHENGWEI NI[2], (Member, IEEE), WANQIU HU[3], AND MEHUL MOTANI[4], (Fellow, IEEE)

[1]Key Laboratory of the Ministry of Education for Optoelectronic Measurement Technology and Instrument, Advanced Equipment Intelligent Perception and Control, Beijing International Cooperation Base for Science and Technology, School of Information and Communication Engineering, Beijing Information Science & Technology University, Beijing 100192, China
[2]School of Information and Electronic Engineering, Zhejiang Gongshang University, Hangzhou 310018, China
[3]School of Information and Communication Engineering, Beijing Information Science & Technology University, Beijing 100192, China
[4]Department of Electrical and Computer Engineering, National University of Singapore, Singapore 117583

Corresponding author: Zhengwei Ni (zhengwei.ni@zjgsu.edu.cn)

This work was supported in part by the Natural Science Foundation of Beijing under Grant 4172021, in part by the Importation and Development of High-Caliber Talents Project of Beijing Municipal Institutions under Grant CIT&TCD 201704064, and in part by the Singapore Ministry of Education under Grant MOE2019-T2-2-171.

ABSTRACT Energy harvesting (EH) relay communication systems with decoding energy costs in multiple block cases have not been widely studied. This paper investigates the relay network with a decode-and-forward relay powered by EH. Unlike other works, we consider the relay with energy decoding costs which harvests random energy from both a dedicated transmitter and other ambient radio-frequency (RF) sources. The EH relay adopts a harvest-receive-forward time-switching architecture. We optimize the time fractions of the three phases and the reception rate at the relay to maximize the offline throughput for single and multiple block cases under two EH scenarios. The multi-block optimization problem constitutes a complex non-convex problem, which we decouple into a single block problem with two auxiliary variables determined by an outer optimization problem. The original problem is finally solved at the cost of linear optimization after series of tricks. Several conclusions are derived: (i) energy storage is necessary (unnecessary) when the relay harvests energy from the transmitter (ambient RF sources), (ii) the optimal reception rate remains unchanged, while the optimal time fractions vary with the energy harvested from ambient RF sources leading to different average throughput. We give numerical simulations to verify our theoretical analysis.

INDEX TERMS Energy harvesting, harvest-receive-forward, relay network, decoding energy, multiple blocks (slots).

I. INTRODUCTION

Practical communication systems with energy harvesting (EH) capabilities are expected to become ubiquitous with the rapid development of Internet of Things (IoT) networks. The EH communication system could be widely used in IoT network [3], vehicle area network, body area network, home area network, wireless sensor network [4], [5], industrial monitoring networks, cognitive-radio network [6] and so on. For example, an EH device can act as a Road Side Unit (RSU), which helps to relay information of vehicles to faraway stations or other nearby vehicles [7]. Another application example is in the fog computing scenario; an EH device can act as a relay, which can help other devices to forward information to the network edge (e.g. IoT gateway). The harvested energy, which can be used to replenish the battery of an IoT node, can be from natural sources (e.g. solar) and human-made sources, such as dedicated and stray radio-frequency (RF) signals. As such, it is important to study optimal energy utilization and communication mechanisms to improve system performance. In these studies, various objectives, such as maximization of throughput [8],

The associate editor coordinating the review of this manuscript and approving it for publication was Eklas Hossain.

energy efficiency [9], minimization of outage probabilities [10], [11], transmission delays [12] and packet drop rate [13], [14] have been considered.

Since IoT devices are expected to be deployed in large numbers, small form factor, low cost and low energy consumption of them are three of the most important design goals. For such a low-power communication system, the decoding cost for information reception is non-negligible. In this work, we consider a throughput maximization problem in a relay network with an EH relay using the decode-and-forward (DF) technique considering decoding costs. The DF technique can suppress the influence of noise better than the amplify-and-forward (AF) technique. In the below, we briefly survey the relevant existing literature.

For relay systems, Huang and Ansari [15] study the scenario when the transmitter node (TX) harvests energy from RF signals transmitted by the relay node (RN), and then they derived optimal solutions for the joint TX and RN power allocation to maximize the overall throughput. Peng *et al.* [16] and Nasir *et al.* [17] have studied when the RN harvests energy from the RF signal of the TX, the optimal power allocation scheme with the power splitting (PS) relay protocol to maximize the throughput. Some studies give the optimal static PS and time allocation ratios for a DF relay network in terms of outage performance and ergodic performance with a 'harvest-then-forward' strategy [18], or in terms of the delay limited and delay-tolerant throughput [8]. Blagojevi *et al.* [19] analyze the performance of the EH DF relay system in generalized-K fading environment. Abedi *et al.* [20] study PS-based relay system with decoding cost, which is a generalized increasing function of the reception rate. Tutuncuoglu *et al.* [21] use a generalized iterative directional water-filling algorithm to solve the sum-rate maximization problem under half-duplex and full-duplex channels with energy harvesting nodes under any relaying strategy, namely DF, AF, compress-and-forward and compute-and-forward. Shi *et al.* [22] analyze the outage performance for a three-step two way EH DF relaying system. Ju and Yang [23] and Van *et al.* [24] both study the two way DF EH relay networks to derive optimum PS coefficients and optimum time-switching (TS) coefficients to maximize the throughput. Rao *et al.* [25] derive the delay-limited and delay-tolerant throughput for a DF single-way and two-way relaying networks with a TS relaying protocol. Zou *et al.* [26] study the joint PS and relay selection in EH communication system in IoT systems.

Reshma and Babu [27] propose an EH based incremental relaying cooperative non-orthogonal multiple access (IR-EH-NOMA) protocol, and derive analytical expressions for the system throughput of IR-EH-NOMA network, which is proved to be superior to conventional cooperative relaying NOMA network with EH (CR-EH-NOMA network) in terms of outage and throughput. Lan *et al.* [28] consider a wireless powered cooperative non-orthogonal multiple access (NOMA) relay network, in which one source is supposed to send independent messages to two users with the assistance of one energy-constrained relay that harvests energy from the source.

For energy efficiency (EE), there are several papers, many of which consider the static power consumption of the transmission circuit. Guo *et al.* [29] give the performance analysis of cooperative NOMA with energy harvesting in multi-cell networks, showing that the energy harvesting enabled cooperative NOMA system in a multi-cell network can improve the coverage probability, ergodic rate, and EE compared to its counterpart orthogonal multiple access (OMA) systems. Zhang *et al.* [30] discuss the EE optimization of AF based energy harvesting two-way relaying systems. utilizing the statistical channel state information, they first build a statistical EE model, which applies to practical environments under fast fading channels. Then, a power allocation problem is formulated to maximize the EE under the constraints of total power and sum rate. Zhao *et al.* [31] consider data transmission in a DF relay-assisted network in which the relay is EH powered while the base station (BS) is power-grid powered. They also compare the EE of an EH relay system with a power-grid powered one and provide more insight into the EE problem. When the harvest-then-use mode is adopted, the non-ideal efficiency of the battery is often discussed. Some papers just use an energy conversion efficiency factor [27], [32], while some papers further model the internal resistance of the battery to discuss the above problems [33].

In fact, due to the low energy consumption of an EH device in IoT, the decoder is the dominant source of energy consumption during reception [34]. Several papers have discussed the model of the decoding energy cost for receiving information, such as [34]–[36], which model the decoding power as an increasing convex function of the reception rate. Though there are some papers investigating relay systems considering the decoding cost, such as [20], [37]–[43], most of them discuss the situation when the random harvested energy arriving at the source, relay, and destination are independent of each other and are uncontrollable by the nodes [37]–[43]. Few papers studying the EH relay, which can harvest RF energy from the transmitter with PS or TS scheme, have paid attention to the decoding cost. For example, Arafa and Ulukus [37] discuss both one-hop and two-hop DF relaying networks considering the decoding cost at the relays and the receiver with random energy harvested independently at the transmitter, the relays and the receiver. When there is a data buffer in the relay, an inner-outer problem is formed. They solve the inner problem using the results of the single-user fading problem [44], and solve the outer problem using a water-filling algorithm. Almost all of the papers studying EH relays with a TS scheme do not consider the decoding cost [15], [17]–[19], [21], [23]–[25]. Most of the papers studying EH relays with a PS scheme also do not consider the decoding cost [8], [16], [18]–[20], [22]–[24], [26], [45], [46]. As we know, the only previous work considering decoding cost functions in a PS relay network is from [20]. Abedi *et al.* [20] adopt a PS scheme and only considers optimizing the power ratio and transceiving rate in a single block. However, they do not consider the energy harvested from ambient RF sources other than the dedicated TX.

Some papers in our research group have discussed the energy decoding cost at the EH receiver in a point-to-point communication system, and have drawn many conclusions on the system design [33], [35], [36]. Ni and Motani [35] optimize the reception rate and time fraction of energy harvesting with different schemes. Ni and Motani [36] extend the work in [35] to joint optimization of transmission power at the transmitter, reception rate and the time fraction for EH at the receiver in a point-to-point communication system. Ni *et al*. [33] further discuss the dual-path structure of EH receivers considering both the internal resistance of the battery and the decoding cost, which constitutes a complex and difficult problem to deal with.

Ni *et al.* [33], Ni and Motani [35], [36] have studied the optimal TS optimization problems, accounting for decoding energy cost at an EH receiver in a point-to-point communication system; When it comes to a relay, which forwards the received information from the transmitter to the destination without a direct link, it is a very different problem. This is because the harvested energy must be carefully divided into two parts respective for decoding and forwarding the information and the process of EH also takes up part of the total processing time, in an EH system where EH and information transceiving share one antenna and one RF front-end. Information reception and forwarding processes are also interrelated, as the decoded data bits must not be fewer than the forwarded data bits at a relay. The analysis for the TS ratios and the throughput will be more complex, especially when random energy can be harvested from other ambient RF sources, and stored at the relay for use in later blocks to form a multiple-phase problem.

In this paper, we investigate the offline throughput performance of a relay network with a transmitter, an EH decode-and-forward (EH-DF) relay and a receiver without a direct link.The energy required for decoding information, which is a major source of energy consumption at a relay with DF technique [47], [48], has not been well studied for EH relays, especially for the multi-block case at the relay. To use the random energy harvested from ambient RF resources other than the dedicated TX in multi-block case, we use storage at the relay, to more efficiently schedule resources, which is not considered in the previous studies.

We consider two energy harvesting scenarios: (i) EH-I: Energy is harvested from the dedicated TX, and (ii) EH-II: Energy is harvested from the dedicated TX and other ambient RF sources.

In this context, the main contributions of the paper are:

- We adopt a simple time-switching system model to formulate the throughput maximization problem. Considering the decoding cost, we give algorithms to obtain the solutions of the optimum time fractions for the three phases and the reception rate with a single block (SB) setting in both scenarios EH-I and EH-II (Section III).
- We obtain optimal solutions of the optimum three time fractions and the reception rate for maximizing the throughput in multi-block (MB) EH-I scenario considering decoding energy costs with an analysis method of auxiliary problem construction and solution comparison (Section IV-A).
- We formulate a multi-phase non-convex optimization problem for the multiple block (MB) EH-II scenario considering decoding energy costs to maximize the throughput, which is not studied before. We transform it into a single-phase problem with two auxiliary variables determined by an outer optimization problem. The feasible domain of the two auxiliary variables and the solution structure for the receiving rate are derived. The complex problem is finally solved at the cost of convex optimization. We can observe that one of the possible solutions of the optimum time fractions for the three phases and the reception rate is always given with no data flowing between blocks from the derivations to solve the problem (Section IV-B).
- We present extensive numerical results to validate our analysis (Section V) and give several important conclusions about the optimal reception rate and the optimal time fractions in various settings. The optimal reception rate remains unchanged for various SB and MB settings in various EH settings, while the optimal time fractions vary with the energy harvested from ambient RF sources. Design principles have been derived for the system: the energy storage is necessary for the relay; however, the data storage is not necessary for the relay (Section VI).

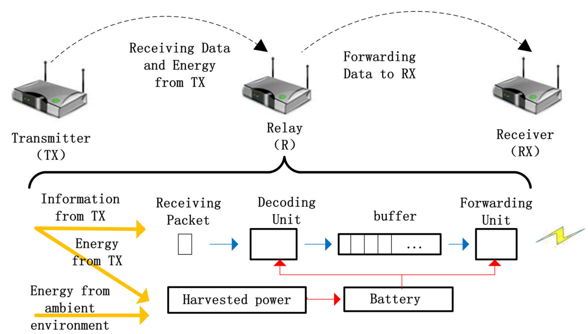

FIGURE 1. Information transmission system with an EH relay.

II. SYSTEM MODEL

We consider an end-to-end relay communication system with a transmitter (TX), a relay node (RN) and a receiver (RX) without a direct link, as shown in Fig. 1. The RN first decodes the signal transmitted by the TX, stores it in the buffer, and then forwards (transmits) it to the RX, using the DF technique. Both the TX and RX are mains-powered. The RN is solely powered by RF signals either from the dedicated TX (Scenario EH-I), or from both the dedicated TX and other ambient RF sources (Scenario EH-II).

In order to simplify the receiver structure, there is one antenna shared by the phases of energy harvesting, receiving and forwarding information with a time-switching on-off controlling the antenna to receive or forward signals. As in [35] using a "Harvest-Then-Receive" time-switching architecture, we consider a "Harvest-Receive-Forward" time-switching architecture in this paper.

We consider a multi-block system, where each block is of τ seconds in length, and is divided into three phases, as shown in Fig. 2. The block structure is elaborated on below.

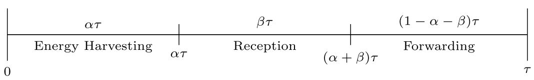

FIGURE 2. The communication block structure at the EH Relay.

- *EH Phase:* Over the time duration $[0, \alpha\tau)$, $\alpha \in [0, 1]$, the switch connects to the EH circuit, and all the signals received are used for harvesting energy. Let p_x be the transmission power with which symbol $x \in \mathcal{X}$ is transmitted, where $\mathcal{X}$ is the set of all possible symbols that the TX can transmit. For the RN to harvest the maximum amount of energy by the end of this phase, the TX should always transmit the symbol $m = \mathrm{argmax}_{x\in\mathcal{X}} p_x$. In fact, sometimes we assume that some energy can be harvested from other ambient RF sources outside the bandwidth of the signal from the dedicated transmitter. Because the energy can be harvested in parallel mode with other operations, it is unnecessary to allocate any time interval in a frame to harvest this part of energy. If energy harvested from other RF sources is considered, we assume that e takes a certain value by accumulation inside one block. However, it may change randomly across different blocks, i.e., there is random e_i for block i in a multi-block case. Such a block-based model for EH especially works well for the cases when the energy arrival process evolves at a slower rate than the data arrival process at the relay [49]–[52]. We note that the duration for which the harvested power can be seen nearly as constant will be in the order of milli-seconds and seconds in RF and PV EH sources, respectively [53], [54]. When the energy arrival process evolves at a fast rate, this model can also work with certain accumulation operations of the arriving energy, probably in a slightly earlier time interval. For example, the accumulation time interval begins from prior to nearly half of the block time, with an extra energy storage needed. In practice, most EH processes, such as the power harvested from PV and RF sources, admit such models [50], [53], [54]. Or without extra storage cost, with fast varying e among blocks, principally, e needs to be predicted only once at the start of the block, with the tiny time taken with a certain precision. In this case, the performance achieved with our model serves as an approximation of the achievable performance with the actual EH process.
- *Reception Phase:* Over the time duration $[\alpha\tau, (\alpha+\beta)\tau)]$, $\alpha+\beta \in [0, 1]$, the switch connects to the information extracting circuit. It is known from [34] that the decoder is the dominant source of energy consumption during the reception. Hence, we only account for the decoding energy required during the reception at the RN. We adopt the same system model as in [34]. For fixed channel capacity C, the power consumed for decoding a codeword with rate R is a non-decreasing convex function of R, i.e., $g(R) = \mathcal{E}_{\mathrm{D}}(\frac{C}{C-R})$, where $g(0) = 0$ [35]. $\frac{C}{C-R}\log_2(\frac{C}{C-R})$ and $(\frac{C}{C-R})^2\log_2^3(\frac{C}{C-R})$ are two common instances for function $\mathcal{E}_{\mathrm{D}}(\frac{C}{C-R})$ [34]. All the other factors are 'hidden' in this function. For example, the channel effect in the reception phase is hidden in the channel capacity C. The total number of bits decoded by the relay in this phase is $I_R = \beta\tau R$ and they are stored in the buffer for later forwarding. In this phase, no energy is harvested.
- *Forwarding Phase:* Over the time duration $[(\alpha+\beta)\tau, \tau]$, the switch connects to the forwarding circuit and the decoded information is forwarded from the RN to the RX. We assume that the communication channel between the RN and the RX is a fading channel with channel power gain h and that the signal is corrupted by additive white Gaussian noise (AWGN) with unit power spectral density. In this case, we consider the average rate as $T(p_t) = 0.5\,B\log(1 + hp_t)$ bps when the forwarding power is p_t. We assume that h is known at the start of a communication block. The total number of bits that can be reliably forwarded is given by $I_T = \gamma\tau T(p_t)$ during the block, where $\gamma = 1 - (\alpha+\beta)$. In this phase, similar to the reception phase, no energy is harvested.

Zhou et al. [55] and Huang and Tu [56] both discuss the fading channel and harvest-store-use cases, but neither of them discusses the direct link case. Di et al. [57] and Huang and Tu [58] both discuss the cooperative transmission with both the relay and direct link and fading channel cases. Di et al. [57] don't consider the harvest-store-use case, while Huang and Tu [58] discuss the harvest-store-use case. None of them discuss the decoding energy cost. This shows that these papers do not discuss all the cases in the relay network optimization.

Our paper does not consider a direct link because the distance between source and destination may be too far, with a similar case setting as in [55] and [56]. The main novelty of our paper is that it considers the decoding cost at a relay in a DF relay network. As we know, it is the first paper discussing decoding cost at an EH relay. Moreover, as there are many new considerations, such as the multi-block case and the multi-source energy harvesting scenario where an EH relay harvests both from the source node and the ambient environment, the paper does not consider the fading factors in this paper temporarily due to the problem complexity. The parameters to be optimized include optimal lengths of the above three phases and the reception rate in each block, whose number is so large, and later we will show that the problem in our paper considering energy decoding cost at an EH relay in a multi-block case with an EH setting of harvesting energy from other ambient RF sources in addition to from dedicated TX, will form a complex multi-phase non-convex problem. As it is a case that has never been discussed before and it is complex enough already, we do not further discuss the problem under fast-fading channels temporarily. Thus, this paper generally discusses the relay network with very slow changing fading conditions. The slow or fast- changing speeds for the channels are defined with respect to the time length of a block. Under a relative slow fading condition, the channel condition can be seen as unchanged approximately during a block or several blocks.

With the above system model, our goal is to find the optimal lengths of the above three phases and the reception rate of the relay such that the total number of bits transmitted from the TX to the RX is maximized in a given period of time. Generally, the relay will perform as a time-slotted or block-based system. When we want to optimize the mean throughput performance in a period longer than one block, there are two distinct cases. The first one is when the energy and data are not allowed to flow to later blocks for use, denoted as the single block case, while the other one is when the energy and data are allowed to flow to later blocks for use, denoted as the multi-block case. We begin with the single block case in the following section.

III. SINGLE BLOCK CASE

In this case, to maximize the number of bits relayed we need to solve the following optimization problem.

A. ENERGY HARVESTED FROM TX ONLY (EH-I)

In this case, maximizing the number of bits relayed is equivalent to solving the following optimization problem.

$$\begin{aligned}
&(\mathrm{P1}) \max_{\alpha,\beta,\gamma,R} I_T,\\
&\text{s.t. } I_R \geq I_T,\\
&\quad \beta\mathcal{E}_{\mathrm{D}}(\frac{C}{C-R}) + \gamma p_t \leq \alpha p_m,\\
&\quad 0 \leq \alpha, \beta, \gamma \leq 1,\\
&\quad 0 \leq \beta \leq 1,\\
&\quad \alpha+\beta+\gamma = 1,\\
&\quad 0 \leq R < C. \qquad (1)
\end{aligned}$$

The first constraint in (P1) follows because the number of bits the relay can forward must be smaller than or equal to the number of bits it has decoded. The second constraint in (P1) follows because the total amount of energy used for receiving and forwarding information in a block must be less than that has been harvested. The physical significance of the other constraints is apparent. To solve (P1), we first give two useful lemmas.

Lemma 1: For the optimal solution to (P1), the first constraint in (1) *must hold with equality, i.e.,*

$$(1-\alpha-\gamma)\tau R = \gamma\tau T(p_t). \qquad (2)$$

Proof: If the equality in (2) does not hold, one can increase γ and decrease β to make the equality hold. When α, R and p_t are fixed, increasing γ means increasing the value of the objective function I_T. □

Lemma 2: For the optimal solution to (P1), the second constraint in (1) *must hold with equality, i.e.,*

$$\beta\mathcal{E}_{\mathrm{D}}(\frac{C}{C-R}) + \gamma p_t = (1-\beta-\gamma)p_m. \qquad (3)$$

Proof: If the equality in (3) does not hold, one can increase γ and decrease α to make the equality hold. When R, β and p_t are fixed, increasing γ means increasing the value of the objective function I_T. □

Based on Lemmas 1 and 2, we can express α and β in terms of R and p_t as

$$\alpha = 1-\beta-\frac{\beta R}{T(p_t)}, \qquad (4)$$

$$\beta = \frac{p_m T(p_t)}{R(p_m+p_t)+(p_m+\mathcal{E}_{\mathrm{D}}(\frac{C}{C-R}))T(p_t)}. \qquad (5)$$

Expressing β and the objective function in (1) in terms of R and p_t, we can rewrite the objective function of (P1) as $\mathcal{O}_1(R) = \beta R\ \tau$. Taking the derivative of $\mathcal{O}_1(R)$ with respect to R, we have $\frac{\partial\mathcal{O}_1}{\partial R} = p_m\tau T(p_t)\mathcal{P}_1(R)$, where $\mathcal{P}_1(R) = \frac{R}{R(p_m+p_t)+(\mathcal{E}_{\mathrm{D}}(\frac{C}{C-R})+p_m)T(p_t)}$. In the following theorem, we derive the properties for a general form of $\mathcal{E}_{\mathrm{D}}(\frac{C}{C-R})$. The proof of Theorem 1 is given in Appendix VI-A.

Theorem 1: Suppose $\mathcal{E}_{\mathrm{D}}(\frac{C}{C-R}) = (\frac{C}{C-R})^m \log^n(\frac{C}{C-R})$, *where* m *and* n *are positive integers. Then we have* $\lim_{R\to 0}\frac{\partial\mathcal{P}_1(R)}{\partial R} > 0$, $\lim_{R\to C}\frac{\partial\mathcal{P}_1(R)}{\partial R}| < 0$. *We have for all* $0 \leq R < C$, $\frac{\partial^2\mathcal{P}_1(R)}{\partial R^2} \leq 0$.

So there is a single R^* maximizing $\mathcal{O}_1(R)$. We will obtain the optimum α^*, β^* and γ^* according to

$$\gamma^* = \frac{R^* p_m}{(p_m+p_t)R^* + T(p_t)(p_m+\mathcal{E}_{\mathrm{D}}(\frac{C}{C-R^*}))},$$

$$\beta^* = \frac{T(p_t)p_m}{(p_m+p_t)R^* + T(p_t)(p_m+\mathcal{E}_{\mathrm{D}}(\frac{C}{C-R^*}))},$$

and $\alpha^* = 1-\beta^*-\gamma^*$.

B. ENERGY HARVESTED FROM TX AND OTHER AMBIENT RF SOURCES (EH-II)

In this subsection, we consider the case when the receiver harvests energy from both the TX and other ambient RF sources. The corresponding optimization problem is given by (P2).

$$\begin{aligned}
&(\mathrm{P2}) \max_{\alpha,\beta,\gamma,R} I_T,\\
&\text{s.t. } I_R \geq I_T, \tau\beta\mathcal{E}_{\mathrm{D}}(\frac{C}{C-R}) + \tau\gamma p_t \leq \alpha p_{\mathrm{m}}\tau + e,\\
&\quad 0 \leq \alpha, \beta, \gamma \leq 1, \alpha+\beta+\gamma = 1, 0 \leq R < C. \qquad (6)
\end{aligned}$$

We show the solution to problem (P2) in the following lemma.

Lemma 3: The optimal solution R^* to (P2) is given by $\frac{\partial \mathcal{P}_2(R)}{\partial R} = 0$, which is the same with (P1). The optimum α^*, β^* and γ^* can be obtained with (7), (8) *and* (9) *when $e \leq \tilde{e}$; otherwise, α^*, β^* and γ^* can be obtained with* (7), (8) *and* (9) *with $e = \tilde{e}$, when $e > \tilde{e}$.*

$$\gamma^* = \frac{R^*(p_m\tau + e)}{(p_m + p_t)R^*\tau + T(p_t)\tau(p_m + \mathcal{E}_{\mathrm{D}}(\frac{C}{C-R^*}))}, \quad (7)$$

$$\beta^* = \frac{T(p_t)(p_m\tau + e)}{(p_m + p_t)R^*\tau + T(p_t)\tau(p_m + \mathcal{E}_{\mathrm{D}}(\frac{C}{C-R^*}))}, \quad (8)$$

$$\alpha^* = 1 - \beta^* - \gamma^*. \quad (9)$$

$$\tilde{e} = \frac{\tau\left(p_t R^* + T(p_t)\mathcal{E}_{\mathrm{D}}(\frac{C}{C-R^*})\right)}{T(p_t) + R^*} \quad (10)$$

Proof: Similar to the analysis of Lemmas 1 and 2, we have

$$\alpha = 1 - \beta - \frac{\beta R}{T(p_t)}, \quad (11)$$

$$\beta = \frac{(p_m\tau + e)T(p_t)}{R(p_m + p_t)\tau + (p_m + \mathcal{E}_{\mathrm{D}}(\frac{C}{C-R}))T(p_t)\tau}. \quad (12)$$

We can rewrite the objective function for problem (P2) as $\mathcal{O}_2(R) = \beta R\tau$. Take the derivative of $\mathcal{O}_2(R)$ with respect to R, we have $\frac{\partial \mathcal{O}_2}{\partial R} = (p_m\tau + e)T(p_t)\mathcal{P}_2(R)$, where $\mathcal{P}_2(R) = \mathcal{P}_1(R)$. According to Theorem 1, there is a single R^* maximizing $\mathcal{O}_2(R)$. We will get the optimum α^*, β^* and γ^* according to (7), (8) and (9).

We could easily find that when e increases, both β and γ will increase, while α will decrease. When α decreases to zero, the energy harvested from ambient RF sources is enough for the relay, which is $\tilde{e}$ in (10) derived from $\beta + \gamma = 1$. □

We give the following Remark to give an intuitive explanation to Lemma 3.

Remark 1: Intuitively, the energy harvesting fraction decreases with the increase of e to allow for more time for reception and forwarding. When α reduces to zero, the energy harvested from ambient RF sources is enough, β and γ are constant values given by (7) *and* (8) *with $e = \tilde{e}$.*

IV. MULTI-BLOCK CASE

We now consider the multi-block case with N blocks. We assume that the channel power gain h remains constant in all the N blocks. We denote the amount of harvested energy from ambient RF sources in block i as e_i units for $i = 1, \ldots, N$. Further, α_i, β_i, γ_i, and R_i denote the time fraction of the EH, reception and forwarding phases, and the rate of communication from the transmitter to the relay in block i, respectively.

A. ENERGY HARVESTED FROM TX ONLY (SCENARIO EH-I)

Now, we first consider when energy and data are allowed to be stored and used in later blocks in the EH-I setting. maximizing the total number of bits delivered in N blocks, is equivalent to solving the following optimization problem:

$$\begin{aligned}
\text{(P3)} \quad &\max_{\boldsymbol{\alpha},\boldsymbol{\beta},\boldsymbol{\gamma},\mathbf{R}} \sum_{i=1}^{N} I_{T_i},\\
\text{s.t.} \quad &\sum_{j=1}^{i} I_{R_j} \geq \sum_{j=1}^{i} I_{T_j},\\
&\sum_{j=1}^{i} I_{T_j} = \sum_{j=1}^{i} T(p_t)\gamma_j\tau,\\
&\sum_{j=1}^{i} I_{R_j} = \sum_{j=1}^{i} R_j\beta_j\tau,\\
&\sum_{j=1}^{i} \alpha_j p_{\mathrm{m}} \geq \sum_{j=1}^{i} \left[p_t\gamma_j + \beta_j\mathcal{E}_{\mathrm{D}}(\frac{C}{C-R_j})\right],\\
&0 \leq \alpha_i \leq 1, 0 \leq \beta_i \leq 1, 0 \leq \gamma_i \leq 1,\\
&\alpha_i + \beta_i + \gamma_i = 1, 0 \leq R_i < C, \quad i = 1, \ldots, N. \quad (13)
\end{aligned}$$

where $\boldsymbol{\alpha} = \{\alpha_1, \ldots, \alpha_N\}$, $\boldsymbol{\beta} = \{\beta_1, \ldots, \beta_N\}$, $\boldsymbol{\gamma} = \{\gamma_1, \ldots, \gamma_N\}$ and $\mathbf{R} = \{R_1, \ldots, R_N\}$. Note that (13) is not a convex optimization problem. We now construct the following optimization problem:

$$\begin{aligned}
\text{(P4)} \quad &\max_{\boldsymbol{\alpha},\boldsymbol{\beta},\boldsymbol{\gamma},\mathbf{R}} \sum_{i=1}^{N} I_{T_i},\\
\text{s.t.} \quad &\sum_{j=1}^{i} I_{R_j} \geq \sum_{j=1}^{i} I_{T_j},\\
&\sum_{j=1}^{i} I_{T_j} = \sum_{j=1}^{i} T(p_t)\gamma_j\tau,\\
&\sum_{j=1}^{i} I_{R_j} = \sum_{j=1}^{i} R_j\beta_j\tau,\\
&\sum_{j=1}^{i} \alpha_j p_{\mathrm{m}} \geq \sum_{j=1}^{i} \left[p_t\gamma_j + \beta_j\mathcal{E}_{\mathrm{D}}(\frac{C}{C-R_j})\right],\\
&0 \leq \alpha_i \leq 1, 0 \leq \beta_i \leq 1, 0 \leq \gamma_i \leq 1,\\
&\alpha_i + \beta_i + \gamma_i = 1, 0 \leq R_i < C, \quad i = 1, \ldots, N,\\
&\alpha_1 = \alpha_2 = \cdots = \alpha_N, \ \beta_1 = \beta_2 = \cdots = \beta_N,\\
&\gamma_1 = \gamma_2 = \cdots = \gamma_N, R_1 = R_2 = \cdots = R_N. \quad (14)
\end{aligned}$$

Lemma 4: The optimal solutions to (P3) and (P4) all satisfy $\sum_{i=1}^{N} I_{R_i} = \sum_{i=1}^{N} I_{T_i}$.

Proof: If the equality $\sum_{i=1}^{N} I_{R_i} = \sum_{i=1}^{N} I_{T_i}$ does not hold, one can increase γ_j and decrease β_j to make the equality hold. When R_j, p_t, α_j are fixed, increasing γ_j means increasing the value of the objective function. □

Compared with (P3), one can see that (P4) has more constraints to ensure that the fractions of time used for EH, reception and forwarding in each block are the same. Theorem 2 and Theorem 3 relate the optimization problem (P4)

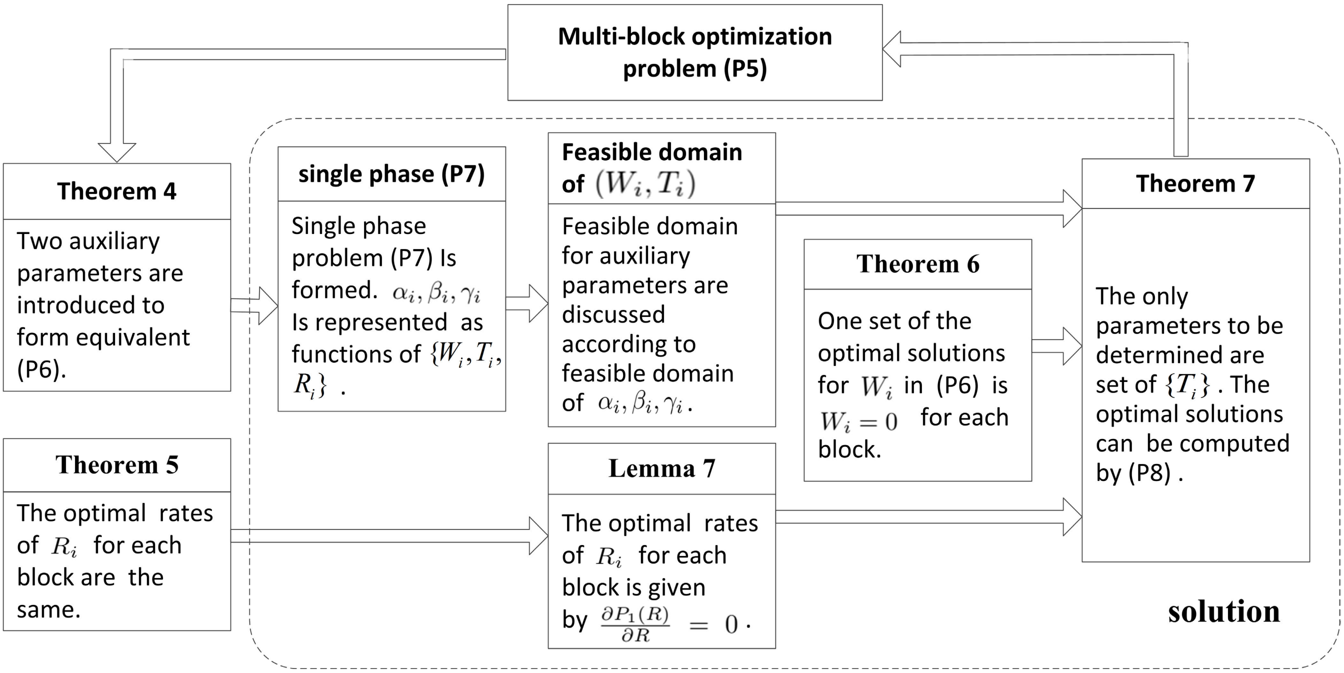

FIGURE 3. Scheme guide map for multi-block problem (P5).

to problem (P1). (14) acts as a bridge between the solutions to (13) and (1).

Theorem 2: The optimal α_i, β_i, γ_i, R_i, $i = 1, \ldots, N$, which maximize the objective function of (14) *are* $\alpha_1 = \cdots \alpha_N = \alpha^*$, $\beta_1 = \cdots \beta_N = \beta^*$, $\gamma_1 = \cdots \gamma_N = \gamma^*$, $R_1 = \cdots R_N = R^*$, *where α^*, β^*, γ^* and R^* are optimal for* (1).

The proof of theorem 2 is given in Appendix VI-B. The following theorem relates the solution to (P4) to that to (P3).

Theorem 3: A set of optimal values for α_i, β_i, γ_i, and R_i, $i = 1, \ldots, N$, which maximize the objective function of (13), *are* $\alpha_1 = \cdots \alpha_N = \alpha^*$, $\beta_1 = \cdots \beta_N = \beta^*$, $\gamma_1 = \cdots \gamma_N = \gamma^*$, $R_1 = \cdots R_N = R^*$, *where α^*, β^*, γ^* and R^* are optimal for* (14).

The proof of Theorem 3 is given in Appendix VI-C. Comparing Theorem 2 with Theorem 3, we find that the relaxation of constraints that the time fractions and code rate in each block are the same cannot improve the performance.

Note that $\boldsymbol{\alpha} = \{\alpha^*, \cdots \alpha^*\}, \boldsymbol{\beta} = \{\beta^*, \cdots \beta^*\}, \boldsymbol{\gamma} = \{\gamma^*, \cdots \gamma^*\}, \boldsymbol{R} = \{R^*, \cdots, R^*\}$ is *a* solution to (P3). There may be other solutions with different time fractions for EH, reception and forwarding phases, and different values of R. To be optimal, the code rates in all the blocks should be equal according to (34).

B. ENERGY HARVESTED FROM TX AND AMBIENT RF SOURCES (SCENARIO EH-II)

In this subsection, we consider the EH scenario when the receiver harvests energy from both the TX and other RF sources, and both energy and data are allowed to flow causally between blocks. The amount of energy harvested from ambient RF sources in the i^{th} block is denoted by e_i. The rest of the assumptions remain the same as in the preceding subsection. In this scenario, maximizing the total number of bits delivered over N blocks is equivalent to solving the following optimization problem:

$$
\begin{aligned}
\text{(P5)}\ & \max_{\boldsymbol{\alpha},\boldsymbol{\beta},\boldsymbol{\gamma},\mathbf{R}} \sum_{i=1}^{N} \gamma_i T(p_t^i)\tau, \\
\text{s.t.}\ & \sum_{j=1}^{i} I_{R_j} \geq \sum_{j=1}^{i} I_{T_j}, I_{R_j} = \beta_j R_j \tau, \\
& \sum_{j=1}^{i} (\alpha_j p_{\mathrm{m}}\tau + e_j) \geq \sum_{j=1}^{i} \left[p_t^j \gamma_j + \beta_j \mathcal{E}_{\mathrm{D}}(\frac{C}{C-R_j}) \right] \tau, \\
& 0 \leq \alpha_i, \beta_i, \gamma_i \leq 1, \alpha_i + \beta_i + \gamma_i = 1, 0 \leq R_i < C, \\
& i = 1, \ldots, N. \qquad (15)
\end{aligned}
$$

where $\boldsymbol{\alpha} = \{\alpha_1, \ldots, \alpha_N\}$, $\boldsymbol{\beta} = \{\beta_1, \ldots, \beta_N\}$, $\boldsymbol{\gamma} = \{\gamma_1, \ldots, \gamma_N\}$ and $\mathbf{R} = \{R_1, \ldots, R_N\}$. Note that (P5) is non-convex.

To solve the problem, we use a series of tricks presented in the third contribution of the paper in Section I. The optimal solution to (P5) is given by Theorem 7. The scheme guide map to obtain the optimal solution to (P5) is shown in Fig. 3.

1) INTRODUCING T_i AND W_i

In order to transform (P5) into an equivalent problem which decouples the blocks, we introduce T_i and W_i as follows

$$T_i = \alpha_i p_m \tau + e_i - (\beta_i \mathcal{E}_{\mathrm{D}}(\frac{C}{C-R_i})\tau + p_t^i \gamma_i \tau), \quad (16)$$

$$W_i = I_{R_i} - I_{T_i}, \quad (17)$$

where T_i denotes the harvested energy minus the used energy in block i, while W_i denotes the received data bits minus the forwarding data in block i. Then we have the following two lemmas.

Lemma 5: $\sum_{k=1}^{i} W_k \geq 0$*, for* $i = 1, 2, \cdots, N$*. To be optimal for (P5),* $\sum_{i=1}^{N} W_i = 0$.

Proof: $\sum_{k=1}^{i} W_k \geq 0$, for $i = 1, 2, \cdots, N$ follows because the forwarded data bits must be less than or equal to the decoded data bits at the relay. $\sum_{i=1}^{N} W_i = 0$ holds because of similar derivations of Lemma 4. □

Lemma 6: $\sum_{k=1}^{i} T_k \geq 0$*, for* $i = 1, 2, \cdots, N$*. To be optimal for (P5), we must minimize* $\sum_{i=1}^{N} T_i$ *subject to* $\sum_{k=1}^{i} T_k \geq 0$.

Proof: $\sum_{k=1}^{i} T_k \geq 0$, for $i = 1, 2, \cdots, N$ follows because the amount of energy consumed must be less than or equal to the amount of energy harvested. If γ_i increases, the objective function will increase accordingly, β_i will increase accordingly and α will decrease accordingly. $\sum T_i$ will of course decrease in this situation. So $\sum T_i$ must be minimized on premise of $\sum_{k=1}^{i} T_k \geq 0$. □

Intuitively, $\sum_{i=1}^{N} T_i$ is the residual energy in the battery at the end of the last block, which should be minimized on premise of effective utilization of energy. At last, we have the following theorem.

Theorem 4: Problem (P5) is equivalent to problem (P6) given by

$$\begin{aligned}
\text{(P6)} \quad & \max_{\boldsymbol{\alpha},\boldsymbol{\beta},\boldsymbol{\gamma},\mathbf{R},\mathbf{T},\mathbf{W}} \sum_{i=1}^{N} I_{T_i} = \sum_{i=1}^{N} \gamma_i T(p_t^i)\tau, \\
& \text{s.t. } I_{R_i} = \beta_i R_i \tau, \\
& \quad \sum_{i=1}^{N} W_i = 0, \\
& \quad \sum_{k=1}^{i} T_k \geq 0, \\
& \quad \sum_{k=1}^{i} W_k \geq 0, \\
& \quad 0 \leq \alpha_i \leq 1,\ 0 \leq \beta_i \leq 1,\ 0 \leq \gamma_i \leq 1, \\
& \quad \alpha_i + \beta_i + \gamma_i = 1, 0 \leq R_i < C, \\
& \quad i = 1, 2, \cdots, N,
\end{aligned}$$

where $\mathbf{T} = \{T_1, \ldots, T_N\}$ *and* $\mathbf{W} = \{W_1, \ldots, W_N\}$.

2) FEASIBLE REGION OF T_i AND W_i

We observe that, for given $\mathbf{T}$ and $\mathbf{W}$, the selection of α_i, β_i, γ_i and R_i is not related to that of α_j, β_j, γ_j, R_j ($i \neq j$), but is only related to T_i and W_i. Hence, for given $\mathbf{T}$ and $\mathbf{W}$, we could decompose the original problem and individually maximize the amount of information in a single block. We can take T_i and W_i as constants for a block that are optimized by an outer optimization problem. Hence, the optimization problem for the i^{th} block can be written as (P7).

$$\begin{aligned}
\text{(P7)} \quad & \max_{\alpha_i,\beta_i,\gamma_i,R_i} I_{T_i} = T(p_t^i)\gamma_i\tau \\
& \text{s.t. } \alpha_i p_m \tau + e_i = \beta_i \mathcal{E}_{\mathrm{D}}\Big(\frac{C}{C - R_i}\Big)\tau + p_t^i \gamma_i \tau + T_i \\
& \quad I_{R_i} = I_{T_i} + W_i, \\
& \quad q20 \leq \alpha_i \leq 1,\ 0 \leq \beta_i \leq 1, \\
& \quad \alpha_i + \beta_i + \gamma_i = 1,\ 0 \leq R_i < C, .
\end{aligned}$$

where T_i and W_i meet (16)-(17), and they can be optimized by an outer optimization problem. We can obtain

$$\alpha_i = 1 - \beta_i + \frac{W_i - \beta_i R_i \tau}{T(p_t^i)\tau}, \tag{18}$$

$$\beta_i = \frac{T(p_t^i)(p_m\tau + e_i - T_i) + W_i(p_m + p_t^i)}{(p_t^i + p_m)R\tau + T(p_t^i)\tau(p_m + \mathcal{E}_{\mathrm{D}}(\frac{C}{C-R_i}))}, \tag{19}$$

$$\gamma_i = \frac{\beta_i R_i \tau - W_i}{T(p_t^i)\tau}. \tag{20}$$

We now consider the feasible region of (W_i, T_i) and discuss how T_i and W_i affect the optimization problem.

The constraints relating to α_i, β_i and γ_i must satisfy
(a) $\beta_i \leq 1$, corresponding to Line 1,
(b) $\beta_i \geq 0$, corresponding to Line 2,
(c) $\beta_i + \gamma_i \leq 1$, corresponding to Line 3,
(d) $\gamma_i \geq 0$, corresponding to Line 4 in Fig. 4.

We next discuss the constraints on T_i and W_i under the four cases (a)-(d).

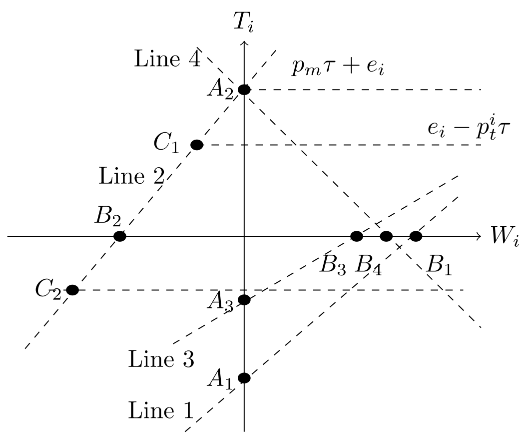

FIGURE 4. Feasible region of (W_i, T_i).

(a) $\beta_i \leq 1$, corresponding to the north-west of Line 1 According to (19), as $\beta_i \leq 1$, we have

$$\begin{aligned}
-T(p_t^i)(\tau\mathcal{E}_{\mathrm{D}}(\frac{C}{C - R_i}) + e_i - T_i) \\
+ (p_t^i + p_m)W_i - (p_t^i + p_m)R_i\tau \leq 0,
\end{aligned} \tag{21}$$

which is denoted in Fig. 4 as the north-west of Line 1. $B_1(R_i\tau + \frac{T(p_t^i)(\tau\mathcal{E}_{\mathrm{D}}(\frac{C}{C-R_i}) - e_i)}{p_t^i + p_m}, 0)$ and $A_1(0, -\frac{(p_m + p_t^i)R_i\tau}{T(p_t^i)})$ are the points on the axes. The slope of Line 1 is $k_1 = -\frac{p_t^i + p_m}{T(p_t^i)}$.

(b) $\beta_i \geq 0$, corresponding to south-east of Line 2

According to (18), as $\beta_i \geq 0$, we have

$$T(p_t^i)(p_m\tau + e_i - T_i) + W_i(p_m + p_t^i) > 0. \tag{22}$$

In Fig. 4, the points on Line 2 represent $\beta_i = 0$ satisfying $T(p_t^i)(p_m\tau + e_i - T_i) + W_i(p_m + p_t^i) = 0$. α_i and γ_i vary with the value of W_i and T_i. $A_2(0, p_m\tau + e_i)$ is one end of the varying process when $\alpha_i = 1, \beta_i = 0, \gamma_i = 0$. C_1 or C_2 is the other end of the varying process when $\beta_i = 0, \gamma_i = 1$. The varying process starts from A_2. When W_i becomes a little smaller, α_i decreases a little and γ_i increases a little, according to (18) and (20) with $\beta_i = 0$, $\alpha_i = 1 - \frac{p_m\tau+e_i-T_i}{(p_m+p_t^i)\tau}$ and $\gamma_i = \frac{p_m\tau+e_i-T_i}{(p_m+p_t^i)\tau}$. $T_i \geq e_i - p_t^i\tau$ is a condition that T_i must satisfy during this varying process. This varying process lasts from A_2 to $T_i = e_i - p_t^i\tau$, $W_i = -T(p_t^i)$, when $\beta_i = 0, \gamma_i = 1$. When $e_i - p_t^i\tau > 0$, Line 2 representing $\beta_i = 0$ starts from A_2 to C_1. When $e_i - p_t^i\tau < 0$, Line 2 representing $\beta_i = 0$ starts from A_2 to C_2. Then $B_2(W_i^2, 0)$ is only in the feasible region when $e_i - p_t^i\tau \leq 0$, where $W_i^2 = -\frac{(p_m+p_t^i)\tau}{T(p_t^i)(p_m\tau+e_i)}$.

(c) $\gamma_i + \beta_i \leq 1$ or $\alpha_i \geq 0$, corresponding to north-west of Line 3

According to (18), as $\beta_i + \gamma_i \leq 1$, we have

$$\begin{aligned} W_i(p_t^i - \mathcal{E}_{\mathrm{D}}(\frac{C}{C-R_i})) - T_i(T(p_t^i) + R_i) \\ + (R_i + T(p_t^i))e_i - (T(p_t^i)\tau e_i + p_t^i R_i\tau) \leq 0. \end{aligned} \tag{23}$$

$B_3(-\frac{(R_i+T(p_t^i))e_i-(T(p_t^i)\tau\mathcal{E}_{\mathrm{D}}(\frac{C}{C-R_i})+p_t^iR_i\tau)}{p_t^i-\mathcal{E}_{\mathrm{D}}(\frac{C}{C-R_i})}, 0)$ and $A_3(0, \frac{(R_i+T(p_t^i))e_i-(T(p_t^i)\tau\mathcal{E}_{\mathrm{D}}(\frac{C}{C-R_i})+p_t^iR_i\tau)}{T(p_t^i)+R_i}$ are the points on the axes for Line 3. The slope of Line 3 is $k_3 = \frac{p_t^i-\mathcal{E}_{\mathrm{D}}(\frac{C}{C-R_i})}{T(p_t^i)+R_i}$. There are four cases for Line 3 in different cases of slopes and intercept A_3.

(d) $\gamma_i \geq 0$, corresponding to the south-west of Line 4

According to (20), as $\gamma_i \geq 0$, we have

$$R_iT_i + W_i(p_m + \mathcal{E}_{\mathrm{D}}(\frac{C}{C-R_i})) \leq (p_m\tau + e_i)R_i, \tag{24}$$

which is denoted in Fig. 4 as Line 4. $B_4(\frac{(p_m\tau+e_i)R_i}{p_m+\mathcal{E}_{\mathrm{D}}(\frac{C}{C-R_i})}, 0)$ and $A_2(0, p_m\tau + e_i)$ are the points on the axes for Line 4. The slope of Line 4 is $k_4 = \frac{p_m+\mathcal{E}_{\mathrm{D}}(\frac{C}{C-R_i})}{R_i}$. For Line 4, A_2 is fixed. B_4 fluctuates a little with the parameters.

It is observed in the feasible region of (W_i, T_i) that there are always positive and negative W_i, but there are not negative T_i sometimes depending on Line 3 and C_2. Later we will show that the objective function relates only to $\{T_i\}$, and $\{W_i = 0\}$ for all i is always one of the optimum solutions.

3) DISCUSSION ABOUT W_i AND R

In this subsection, we will first discuss the solution for R, and then we give possible solutions for W_i. These are prepared for simplifying the optimization problem in Section IV-B4.

Theorem 5: For a fixed average forwarding rate $T(p_t)$, representing with constant p_t and h, for all blocks, the best R_i is the same for all the blocks, i.e., $R^* = \frac{\sum_{i=1}^N \beta_i R_i}{\sum_{i=1}^N \beta_i}$.

The proof of Theorem 5 is given in Appendix D.

Remark 2: When e_i is small, we can always harvest enough energy for information reception at a large enough rate through increasing α_i. When e_i is large enough, we can decrease α_i for information reception and forwarding. When e_i is even larger, the harvested energy can be stored for use in later blocks. Assume there is no limit in energy storage and the data buffer. So the best rate for R_i can always be achieved in all the blocks by adjusting α_i, β_i and γ_i to minimize the total energy for transferring information.

Next, we discuss the optimum value of R^*.

Lemma 7: The optimum value $\mathbf{R}$ for (P6) is $R_i = R^*$, $i = 1, 2, \cdots, N$, satisfying $\frac{\partial P_1(R)}{\partial R} = 0$, where $P_1(R) = \frac{R}{R(p_m+p_t)+T(p_t)(p_m+\mathcal{E}_{\mathrm{D}}(\frac{C}{C-R}))}$.

The proof of Lemma 7 is given in Appendix VI-E. To solve (P6), we discuss the possible value for $\{T_i, W_i\}$. Due to (40), the objective function of (P6) is

$$\begin{aligned} \sum_{i=1}^N \mathcal{O}_6(W_i, T_i) = \sum_{i=1}^N T(p_t) \\ \times \frac{R^*(p_m\tau + e_i - T_i) - W_i(p_m + \mathcal{E}_{\mathrm{D}}(\frac{C}{C-R^*}))}{(p_t + p_m)R^* + T(p_t)(p_m + \mathcal{E}_{\mathrm{D}}(\frac{C}{C-R^*}))}. \end{aligned} \tag{25}$$

Theorem 6: One of the optimum solutions to (P6) is $\sum_{i=1}^N \mathcal{O}_6(0, T_i)$, which means that $W_i = 0$ for each block.

The proof of Theorem 6 is given in Appendix VI-F.

4) SIMPLIFYING THE OPTIMIZATION PROBLEM

So with Theorem 6, together with the feasible regison discussion, we rewrite (P6) as

$$\text{(P8)} \max_{\mathbf{T}} \sum_{i=1}^N \frac{T(p_t)(p_m\tau + e_i - T_i)R}{(p_t + p_m)R + T(p_t)(p_m + \mathcal{E}_{\mathrm{D}}(\frac{C}{C-R}))}$$

$$\text{s.t.} \sum_{k=1}^i T_k \geq 0,$$

$$T_i \geq \frac{(R + T(p_t))e_i - (T(p_t)\tau\mathcal{E}_{\mathrm{D}}(\frac{C}{C-R}) + p_tR\tau)}{T(p_t) + R}, \tag{26}$$

$$T_i \geq -\frac{(p_m + p_t)R\tau}{T(p_t)}, \tag{27}$$

$$T_i \geq e_i - p_t\tau, \tag{28}$$

$$T_i \leq p_m\tau + e_i, i = 1, 2, \cdots, N, \tag{29}$$

where R equals R^* computed according to Lemma 7, (26) follows because A_3 is the lower bound for T_i in case (c), (27) follows because A_1 is the lower bound for T_i in case (a), and (28) follows because C_2 or C_1 is the lower bound for T_i in case (b). (P8) is a linear programming problem with polynomial-time complexity to arbitrary accuracy [59]. The complexity is N^2m, where m is the number of constraints.

After $\mathbf{T}^*$ is determined with (P8), the optimum $\boldsymbol{\alpha}^*, \boldsymbol{\beta}^*, \boldsymbol{\gamma}^*$ could be obtained by (18)-(20). Thus, the solution of (P6) is obtained. Since (P5) is equivalent to (P6), the solution of (P5) is also given by the above optimum $\boldsymbol{\alpha}^*, \boldsymbol{\beta}^*, \boldsymbol{\gamma}^*, \mathbf{R}^*$. So we have the following theorem.

Theorem 7: One of the solution to (P5) is given by $R_i = R^*$ *computed according to Lemma 7,* $W_i^* = 0$, $\gamma_i^* = \frac{R^*(p_m\tau+e_i-T_i^*)}{(p_t+p_m)\tau R^*+T(p_t)\tau(p_m+\mathcal{E}_{\mathrm{D}}(\frac{C}{C-R^*}))}$, $\beta_i^* = \frac{T(p_t)(p_m\tau+e_i-T_i^*)}{(p_t+p_m)\tau R^*+T(p_t)\tau(p_m+\mathcal{E}_{\mathrm{D}}(\frac{C}{C-R^*}))}$, $\alpha_i^* = 1-\beta_i^*-\gamma_i^*$, *for* $i = 1, 2, \cdots, N$, *where* $\mathbf{T}$ *is given by solving the linear programming problem (P8).*

Remark 3: For (P5), $\{W_i = 0\}$, $i = 1, 2, \cdots, N$ *is only one choice for* $\mathbf{W}$. *When* W_i *is within the feasible region, there will be other possible solutions to (P6), with the same optimum value for the objective function as* $\{W_i = 0\}$, $i = 1, 2, \cdots, N$.

V. NUMERICAL RESULTS

In this section, we present simulation results. Although the results are presented for specific parameters to illustrate our approach, the trends are more general and can be observed for other parameters. We assume that $\mathcal{E}_{\mathrm{D}}(\theta) = 10^{-3} \times \theta \log_2 \theta$, $\theta = \frac{C}{C-R}$, $T(p_t) = 0.5\, B \log_2(1 + p_t h')$ bps, $B = 10^6$ Hz, $N_0 = 10^{-15}$ W/Hz, $\tau = 1$ s, $h' = \frac{1}{N_0\, B} = 10^9$. If we adopt energy unit as mJ and bit rate unit as Mbps, we have $\mathcal{E}_{\mathrm{D}}(\theta) = \frac{C}{C-R}\log_2(\frac{C}{C-R})$ mW, $T(p_t) = 0.5\log_2(1+p_t h)$ Mbps, where p_t is forwarding power in mW, and $h = 10^6$. The quantities C, R and $T(p_t)$ are expressed with unit of Mbps.

A. SINGLE BLOCK CASE

We firstly consider the EH-I scenario. Our goal is to find the optimal solution to (P1).

When $p_m = 8$ mW, $p_t = 7$ mW, C=21 Mbps, the optimal R^* must satisfy $\frac{\partial P_1(R)}{\partial R} = 0$. We can compute the optimal R^* to be 14.3630 Mbps by a linear search, and the optimum time fraction of harvesting, reception and forwarding phases are $\alpha = 0.4378$, $\beta = 0.2484$ and $\gamma = 0.3138$, respectively. In order to verify this, we plot the objective function of (P1) in (1) versus R in Fig. 5, from which we can see $R^* = 14.3630$ Mbps. Note that R^* is related only to p_t, p_m and C, and not related with the energy harvested from other ambient RF sources. The optimal throughput rate of the relay network is 3.5678 Mbps.

We also examine the variation of α, β and γ with p_t and p_m in Fig. 6, Fig. 7, and Fig. 8, respectively. We can observe that when p_m, the average power of the best symbol for EH increases, α decreases, while β and γ increase. It is a correct trend as α, the time duration for EH, could be shorter than before, as a result of the increase of p_m. When the forwarding power p_t increases, γ decreases. It is a correct trend because γ, the time duration for forwarding the same amount of data will decrease, and α, the time duration for the EH phase will increase because the forwarding power is less efficient in power as the forwarding data bits I_T are a log function of p_t. For the same reason, β will decrease, too, leading to a lower throughput of the relay network.

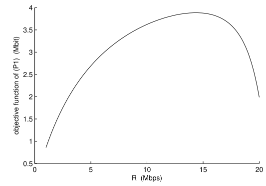

FIGURE 5. The objective function value of (P1) versus R.

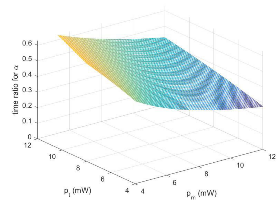

FIGURE 6. α versus p_t and p_m.

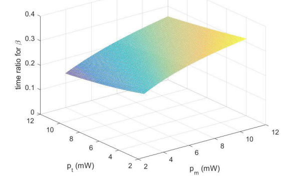

FIGURE 7. β versus p_t and p_m.

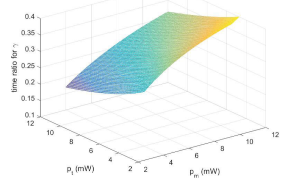

FIGURE 8. γ versus p_t and p_m.

Now we consider the EH-II scenario. According to Lemma 3, when $p_m = 8$ mW, $p_t = 7$ mW, $C = 21$ Mbps, the optimal reception rate for the relay is computed as $R^* = 14.3630$ Mbps from Fig. 5, the same as in the EH-I scenario. We present the variation of optimum α, β and γ versus e in Fig. 9. $\tilde{e}$ is computed to be 6.2303 mJ according to (10) in this case. We can see that β and γ increase with e, but α decreases with e over $e \leq \tilde{e}$; for $e > \tilde{e}$, both α and β no longer vary, but remain the same as when $e = \tilde{e}$. The maximum throughput versus e for the scenario with $p_m = 8$ mW and $p_t = 7$ mW, is computed using $\beta\tau R$ shown in Fig. 10, which is with the same trend of β. When the energy harvested from other ambient RF sources is saturated with $\tilde{e} = 6.2303$ mJ, $\alpha = 0$, $\beta = 0.4418$, $\gamma = 0.5582$, and the throughput rate of the relay network is 6.3456 Mbps.

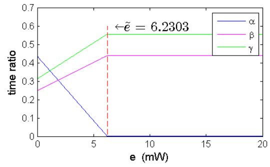

FIGURE 9. The variation of α, β, γ with e.

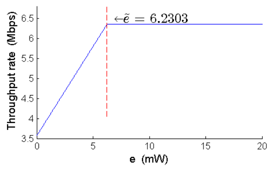

FIGURE 10. The throughput rate versus e.

From these figures, we see the numerical results coincide with the theoretical analysis.

B. MULTI-BLOCK CASE

In this section, we first consider a multi-block case in the EH-I scenario when data and energy are allowed to flow between blocks. According to Theorem 3, one of the possible optimal solutions is given by the optimal solution of the single block case in the EH-I scenario. So for the optimum values for $\mathbf{R}$, $\boldsymbol{\alpha}, \boldsymbol{\beta}, \boldsymbol{\gamma}$, refer to Section V-A for performance analysis, because an optimal solution is the same as the solution of single block case in the EH-I scenario.

We then consider the multi-block case in the EH-II scenario. When $N \geq 1$, the energy harvested from other RF sources in each block is random. We set several scenarios to analyze how e_i will affect the performance of the system. We first set a scenario (Scenario I) when the energy harvested from other ambient RF sources is saturated almost all the time. Then we set a scenario (Scenario II) when e_i is saturated at the first block, and then in the next four blocks, e_i is not saturated. The mean energy of e_i in the five blocks is not saturated. Later we set a scenario (Scenario III) when e_i is not saturated in any of the five blocks, but fluctuates in amount.

All the EH scenarios below in this subsection is with the same system parameters $p_m = 8$ mW, $p_t = 7$ mW, $C = 21$ Mbps. The optimum solution for R^* is given by Lemma 7 by solving $P_1(R) = 0$, as 14.3630 Mbps. And then we obtain the optimum $\boldsymbol{\alpha}^*$, $\boldsymbol{\beta}^*$, $\boldsymbol{\gamma}^*$, $\mathbf{W}^*$, $\mathbf{T}^*$ by Theorem 7 for the following scenarios.

Scenario I: Assume $N = 5$, the harvested energy for blocks is $\mathbf{e} = [10, 9, 8, 12, 10]$ mW. From Theorem 7, we give the solutions as $R_i^* = 14.3630$ Mbps, $W_i^* = 0$ for $i = 1, 2, \cdots, 5$, and $\mathbf{T}^* = [3.7697, 2.7697, 2.7697, 5.7697, 3.7697]$. The optimal $\boldsymbol{\alpha}^*$, $\boldsymbol{\beta}^*$, $\boldsymbol{\gamma}^*$ are given in Fig.11, where $\alpha_i = 0$, $\beta_i = 0.4418$, $\gamma_i = 0.5582$, for all the five blocks. We can observe that when the energy harvested from other RF sources is saturated for the system, i.e., $e_i \geq \tilde{e}$, $i = 1, 2, \cdots, 5$, the EH time ratio is

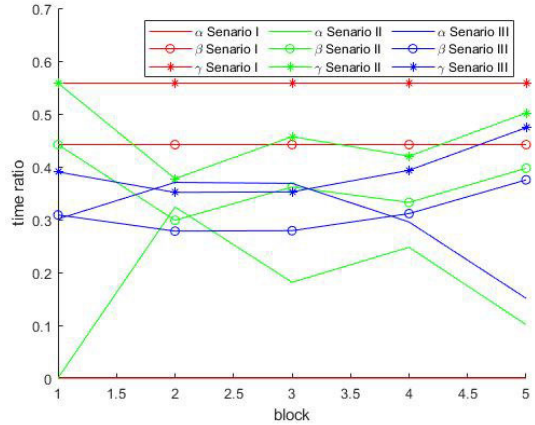

FIGURE 11. The optimal α, β, γ at different blocks in different EH scenarios: Scenario I: $\mathbf{e} = [10, 9, 8, 12, 10]$, Scenario II: $\mathbf{e} = [9, 1, 3, 2, 4]$, Scenario III: $\mathbf{e} = [2, 1, 1, 2, 4]$.

always zero, and β_i and γ_i remain unchanged. $\tilde{e} = 6.2303$ is the saturated energy harvested from other ambient RF sources in single block case as analyzed in Section V-A according to (10). The optimal mean throughput in the five blocks is $\frac{\sum_{i=1}^{5} \beta_i^* R_i^*}{5} = 6.3456$ Mbps, which is the same as in the single block case when the energy harvested from other ambient RF sources e is saturated with $\tilde{e} = 6.2303$ mJ.

Scenario II: Assume $N = 5$, the harvested energy for blocks is $\mathbf{e} = [9, 1, 3, 2, 4]$ mW. From Theorem 7, we give the solutions as $R_i^* = 14.3630$ Mbps, $W_i^* = 0$ for $i = 1, 2, \cdots, 5$, and $\mathbf{T}^* = [2.7697, -0.6219, -0.6500, -0.7064, -0.7913]$. The optimal $\boldsymbol{\alpha}^*, \boldsymbol{\beta}^*, \boldsymbol{\gamma}^*$ are given in Fig. 11. We can observe that the amount of energy harvested from other RF sources is generally large at the beginning and the end of the five block time period, and small in the middle of the period. Since the energy can be stored and used in later blocks, a lot of energy flows to later blocks. α_i has some decreasing trend. β_i and γ_i fluctuate a little in five blocks, with some increasing trend. The optimal mean throughput in the five blocks is $\frac{\sum_{i=1}^{5} \beta_i^* R_i^*}{5} = 5.2626$ Mbps. The average throughput is the same as when the harvested energy from other ambient RF sources is $e = \frac{\sum_{i=1}^{5} e_i}{5}$ in the single block case. If we assume that there is not energy storage, then the energy will overflow in the first block as $e_1 > \tilde{e}$, where $\tilde{e} = 6.2303$ is the saturated energy harvested from other ambient RF sources in the single block case as analyzed in Section V-A according to (10). The average throughput without energy storage will be smaller than the throughput with storage in this case.

Scenario III: Assume $N = 5$, the harvested energy for blocks is $\mathbf{e} = [2, 1, 1, 2, 4]$ mW. From Theorem 7, we give the solutions as $R_i^* = 14.3630$ Mbps, $W_i^* = 0$ for $i = 1, 2, \cdots, 5$, and $\mathbf{T}^* = [0, 0, 0, 0, 0]$. The optimal $\boldsymbol{\alpha}^*, \boldsymbol{\beta}^*, \boldsymbol{\gamma}^*$ are given in Fig. 11. We can observe that the amount of energy harvested from other RF sources generally increases with time in the scenario, which is relatively low with respect to the saturated $\tilde{e}$. So the harvested energy from

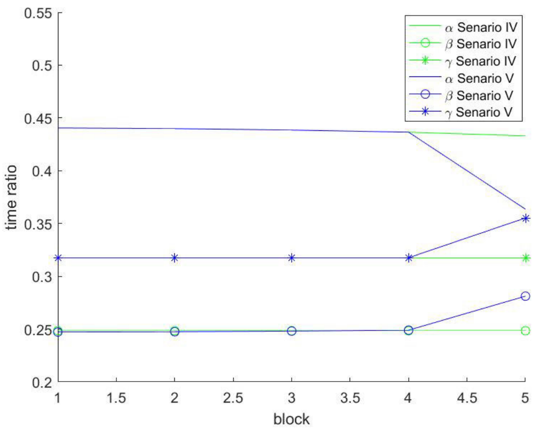

FIGURE 12. The optimal α, β, γ at different blocks in different EH Scenarios: Scenario IV: $e = [0, 0, 0, 0, 0]$, Scenario V: $e = [0, 0, 0, 0, 1]$.

other RF sources is not stored in the battery and is used in immediate blocks. The optimal mean throughput in the five blocks is $\frac{\sum_{i=1}^{5}\beta_i^* R_i^*}{5} = 4.4597$ Mbps.

We can observe from Scenario II, when the energy is ample in the early blocks, the energy generally flows to later blocks, as T has some decreasing trend. We expect that when the energy is too scarce, the energy may also flow to later blocks. To verify this, we give two additional scenarios when the energy harvested from other ambient RF sources is zero all the time and when the energy harvested from other ambient RF sources is zero in the first four blocks but one unit in the last block.

Scenario IV: Assume $N = 5$, the harvested energy for blocks is $\mathbf{e} = [0, 0, 0, 0, 0]$ mW. From Theorem 7, we give the solutions as $R_i^* = 14.3630$ Mbps, $W_i^* = 0$ for $i = 1, 2, \cdots, 5$, and $\mathbf{T}^* = [0.038, 0.0285, 0.0095, -0.0190, -0.0570]$. The optimal $\boldsymbol{\alpha}^*, \boldsymbol{\beta}^*, \boldsymbol{\gamma}^*$ are given in Fig. 12. We can observe that a lot of energy flows to later blocks. α_i has some decreasing trend. β_i and γ_i have some increasing trend. The optimal mean throughput in the five blocks is $\frac{\sum_{i=1}^{5}\beta_i^* R_i^*}{5} = 3.5678$ Mbps, which is the same as in the single block case, when $e = 0$, with $\beta = 0.2484$ and the throughput of 3.5678 Mbps, in Section V-A. This result fits well with our expectation. Though the energy flows to later blocks for use, the average throughput is generally the same as when the energy is used evenly in each of the blocks.

Scenario V: Assume $N = 5$, the harvested energy for blocks is $\mathbf{e} = [0, 0, 0, 0, 1]$ mW. From Theorem 7, we give the solutions as $R_i^* = 14.3630$ Mbps, $W_i^* = 0$ for $i = 1, 2, \cdots, 5$, and $\mathbf{T}^* = [0.0380, 0.0285, 0.0095, -0.0190, -0.0571]$. The optimal $\boldsymbol{\alpha}^*, \boldsymbol{\beta}^*, \boldsymbol{\gamma}^*$ are given in Fig. 12. We can observe that the amount of energy harvested from other RF sources increases only in the last block. Since the energy can be stored and used in later blocks, a lot of energy still flows to later blocks. α_i has some decreasing trend. β_i and γ_i have some increasing trend. The optimal mean throughput in the five blocks is $\frac{\sum_{i=1}^{5}\beta_i^* R_i^*}{5} = 3.6568$ Mbps, which is a little higher than 3.5678 Mbps. In fact, we can observe that the throughput in case of $\mathbf{e} = [0, 0, 0, 0, 1]$ is the same as the throughput when $e = 0.2$ and $\beta = 0.2546$ in a single block case, and it is the same as the average throughput of the separate single block cases when $e = 0, e = 0, e = 0, e = 0, e = 1$, respectively. The result fits well with our expectation. Though the energy flows to later blocks for use, the average throughput is generally the same as when the energy is not allowed to flow.

From the above analysis, we observe that the energy storage takes effect when saturated amount of energy arrives in early blocks and the amount of energy harvested from ambient RF sources is not saturated for all the blocks, such as in Scenario II with multiple block setting. When the energy harvested from ambient environment is not saturated in any of the blocks, the average throughput is the same as when the energy is not allowed to flow, such as in Scenario III, Scenario IV and Scenario V. When e_i is saturated in all the blocks, the average throughput is the same as when the energy is not allowed to flow, such as in Scenario I.

From the analysis, as expected, when the energy from ambient RF sources is considered, the energy storage plays an important role in scheduling the resource to maximize the offline throughput. The data storage is unnecessary from Remark 3. When the harvested energy coming from the ambient sources is considered, the energy utilization efficiency is further increased in the aspect that larger throughput will be achieved with the same amount of energy consumed by the dedicated TX. We do not perform comparisons with other methods because there is not any study in this scenario with both decoding energy cost and storage considered in an EH relay.

VI. CONCLUSION

In this paper, we considered maximizing the offline throughput of a network with an EH-DF relay, which can harvest energy not only from the dedicated transmitter but also from other ambient RF sources considering decoding energy costs, which is not a well-studied topic. In order to make full use of the harvested energy, energy storage is used to allow energy flow between blocks, which is also not well studied in the former works. In order to simplify the system structure, a time-switching architecture is adopted. We formulate a problem for maximizing the throughput by optimizing the time fractions of three phases and the reception rate. From the optimal solutions, we draw the following conclusions:

(i) In the multi-block case, the energy storage is necessary for an EH relay which can harvest energy from RF sources other than the dedicated TX considering the decoding energy cost. However, data storage is not necessary for the relay system. This is one of our important observations; (ii) The optimal reception rate remains unchanged for both single and multiple block cases in various EH scenarios, while the time fractions of the three phases vary with the random energy harvested from other ambient RF sources leading to different average throughput; (iii) For a single-block case with energy harvested from ambient RF sources other than the dedicated TX, the optimal time fractions for reception and forwarding increase with the increase of harvested energy from other ambient RF sources, but with upper bounds. Our future work involves maximization of the offline throughputs of a relay network with random relay-transmitter and transmitter-relay channel power gains.

APPENDIX

A. PROOF OF THEOREM 1

If we use mW as the unit for power and Mbps as the unit for transferring rate, then we could assume $T(x) = 0.5\log_2(1+hx)$, where $h = 10^6$. We could derive $\frac{\partial \mathcal{P}_1(R)}{\partial R} = \frac{T(p_t)(\mathcal{E}_D(\theta)+p_m)-T(p_t)\frac{\partial \mathcal{E}_D(\theta)}{\partial\theta}\frac{R}{(C-R)^2}}{[R(p_m+p_t)+(\mathcal{E}_D(\theta)+p_m)T(p_t)]^2}$, and $\frac{\partial^2\mathcal{P}_1(R)}{\partial R^2} = -RT(p_t)\frac{\frac{\partial^2\mathcal{E}_D(\theta)}{\partial\theta^2}\frac{1}{(C-R)^4}+2\frac{\partial\mathcal{E}_D(\theta)}{\partial\theta}\frac{1}{(C-R)^3}}{[R(p_m+p_t)+(\mathcal{E}_D(\theta)+p_m)T(p_t)]^4}$, where $\theta = \frac{C}{C-R}$. For $\mathcal{E}_D(\theta) = \theta^m\log^n\theta$, we could derive $\frac{\partial\mathcal{E}_D(\theta)}{\partial\theta} = \theta^{m-1}\log^{n-1}\theta[mlog\theta + n/ln2]$, $\lim_{R\to 0}\theta = 1$ and $\lim_{R\to C}\theta = +\infty$. So $\lim_{\theta\to 1}\frac{\partial\mathcal{P}_1}{\partial R} = \lim_{\theta\to 1}\frac{T(p_t)p_m+T(p_t)\left[\theta^m\log^{n-1}\theta[1-\theta(\theta-1)(m\log\theta+n/ln2)/C]\right]}{T^2(p_t)R^2(p_m+p_t)^2} = \frac{p_m}{T(p_t)R^2(p_m+p_t)^2}$, whose denominator and numerator are both finite. So $\lim_{\theta\to 1}\frac{\partial\mathcal{P}_1}{\partial R}$ is positive finite. $\lim_{\theta\to+\infty}\frac{\partial\mathcal{P}_1}{\partial R} = \lim_{\theta\to+\infty} -\frac{\theta^{m-1}(\log^{n-1}\theta)\theta(\theta-1)(m\log\theta+n/ln2)/C}{T(p_t)\theta^{2m}\log^{2n}\theta} = \lim_{\theta\to+\infty} -\frac{m/C}{T(p_t)\theta^{m-1}\log^{n-1}\theta} < 0$. $\frac{\partial^2\mathcal{P}_1(R)}{\partial R^2}$ could easily be seen as nonpositive for $R\in[0,C)$.

B. PROOF OF THEOREM 2

We argue that $\alpha_1 = \cdots\alpha_N = \alpha^*$, $\beta_1 = \cdots\beta_N = \beta^*$, $\gamma_1 = \cdots = \gamma_N = \gamma^*$, $R_1 = \cdots R_N = R^*$ satisfy the first eight constraints in (P4), i.e., all the constraints in (P3), since

$$\begin{aligned}\alpha^* p_m &= \beta^*\mathcal{E}_D(\frac{C}{C-R^*})+\gamma^* p_t\\ \Leftrightarrow \sum_{j=1}^{i}\alpha^* p_m &= \sum_{j=1}^{i}\left[\beta^*\mathcal{E}_D(\frac{C}{C-R^*})+\gamma^* p_t\right],\\ \Rightarrow \sum_{j=1}^{i}\alpha^* p_m &\geq \sum_{j=1}^{i}\left[\beta^*\mathcal{E}_D(\frac{C}{C-R^*})+\gamma^* p_t\right],\\ &\text{for } i=1,2,\cdots,N,\end{aligned}\tag{30}$$

$$\begin{aligned}\beta^*R^*\tau &= \gamma^*T(p_t)\tau \Leftrightarrow \sum_{j=1}^{i}\beta^*R^*\tau = \sum_{j=1}^{i}\gamma^*T(p_t)\tau,\\ &\Rightarrow \sum_{j=1}^{i}\beta^*R^*\tau \geq \sum_{j=1}^{i}\gamma^*T(p_t)\tau,\\ &\text{for } i=1,2,\cdots,N.\end{aligned}\tag{31}$$

It is obvious that the last four equations in (P4) are also satisfied. We will prove the optimality via contradiction. Define $\mathcal{O}_N(\alpha_1,\beta_1,\gamma_1,R_1\ldots,\alpha_N,\beta_N,\gamma_N,R_N) = \sum_{i=1}^{N}\gamma_i T(p_t^i)\tau$. Suppose there exists another set of $\hat{\alpha}$, $\hat{\beta}$, $\hat{\gamma}$ and $\hat{R}$ such that when $\alpha_1 = \cdots\alpha_N = \hat{\alpha}$, $\beta_1 = \cdots\beta_N = \hat{\beta}$, $\gamma_1 = \cdots\gamma_N = \hat{\gamma}$ and $R_1 = \cdots R_N = \hat{R}$, all the constraints of (14) are satisfied and we have $\mathcal{O}_N(\hat{\alpha},\hat{\beta},\hat{\gamma},\hat{R}\ldots,\hat{\alpha},\hat{\beta},\hat{\gamma},\hat{R}) > \mathcal{O}_N(\alpha^*,\beta^*,\gamma^*,R^*\ldots,\alpha^*,\beta^*,\gamma^*,R^*)$, i.e., $N\hat{\beta}\hat{R}\tau > N\beta^*R^*\tau$. Since it is always optimal to use up all the energy in the end, according to the constraints, we have $N\hat{\alpha}p_m = N\hat{\gamma}p_t + N\hat{\beta}\mathcal{E}_D(\frac{C}{C-\hat{R}})$, which means $\hat{\alpha}$, $\hat{\beta}$, $\hat{\gamma}$ and $\hat{R}$ also satisfy the constraints of (1).

Since $\hat{\beta}\hat{R}\tau > \beta^*R^*\tau$, the results contradict the assumption that α^*, β^*, R^* and γ^* are the optimal values for (1).

C. PROOF OF THEOREM 3

Since (P4) has four more constraints than (P3), assuming one set of optimal values for (P3) are given as $\tilde{\alpha}_1,\tilde{\beta}_1,\tilde{\gamma}_1,\tilde{R}_1,\ldots,\tilde{\alpha}_N,\tilde{\beta}_N,\tilde{\gamma}_N,\tilde{R}_N$, it is easy to obtain

$$\begin{aligned}&\mathcal{O}_N(\tilde{\alpha}_1,\tilde{\beta}_1,\tilde{\gamma}_1,\tilde{R}_1,\ldots,\tilde{\alpha}_N,\tilde{\beta}_N,\tilde{\gamma}_N,\tilde{R}_N)\\ &\quad\geq \mathcal{O}_N(\alpha^*,\beta^*,\gamma^*,R^*,\ldots,\alpha^*,\beta^*,\gamma^*,R^*).\end{aligned}\tag{32}$$

Due to the property of $\mathcal{E}_D(\frac{C}{C-R})$, by using Jensen's inequality to code rate, we have

$$\sum_{j=1}^{N}\frac{\tilde{\beta}_j}{\Phi}\mathcal{E}_D\left(\frac{1}{1-\frac{\tilde{R}_j}{C}}\right) \geq \mathcal{E}_D\left(\frac{1}{1-\sum_{j=1}^{N}\frac{\tilde{\beta}_j}{\Phi}\tilde{R}_j/C}\right),\tag{33}$$

where $\Phi = \sum_{k=1}^{N}\tilde{\beta}_k$. Hence, we arrive at

$$\begin{aligned}\sum_{j=1}^{N}\tilde{\alpha}_j p_m &= \sum_{j=1}^{N}\tilde{\beta}_j\mathcal{E}_D\left(\frac{1}{1-\frac{\tilde{R}_j}{C}}\right)+\sum_{j=1}^{N}\tilde{\gamma}_j p_t\\ &\geq \sum_{j=1}^{N}\tilde{\beta}_j\mathcal{E}_D\left(\frac{1}{1-\frac{\sum_{k=1}^{N}\tilde{\beta}_k\tilde{R}_k}{\sum_{k=1}^{N}\tilde{\beta}_k C}}\right)+\sum_{j=1}^{N}\tilde{\gamma}_j p_t.\end{aligned}$$

So there exists an $R' \geq \frac{\sum_{k=1}^{N}\tilde{\beta}_k\tilde{R}_k}{\sum_{k=1}^{N}\tilde{\beta}_k}$ that satisfies $\sum_{j=1}^{N}\tilde{\alpha}_j p_m = \sum_{j=1}^{N}\tilde{\beta}_j\mathcal{E}_D\left(\frac{1}{1-\frac{R'}{C}}\right)+\sum_{j=1}^{N}\tilde{\gamma}_j p_t$. Actually, $R' \geq \frac{\sum_{k=1}^{N}\tilde{\beta}_k\tilde{R}_k}{\sum_{k=1}^{N}\tilde{\beta}_k}$ means

$$\begin{aligned}&\mathcal{O}_N(\tilde{\alpha}_1,\tilde{\beta}_1,\tilde{\gamma}_1,R',\ldots,\tilde{\alpha}_N,\tilde{\beta}_N,\tilde{\gamma}_N,R')\\ &\quad\geq \mathcal{O}_N(\tilde{\alpha}_1,\tilde{\beta}_1,\tilde{\gamma}_1,\tilde{R}_1,\ldots,\tilde{\alpha}_N,\tilde{\beta}_N,\tilde{\gamma}_N,\tilde{R}_N).\end{aligned}\tag{34}$$

However, this new R' alongside $\tilde{\alpha}_1,\ldots,\tilde{\alpha}_N$, $\tilde{\beta}_1,\ldots,\tilde{\beta}_N$ and $\tilde{\gamma}_1,\ldots,\tilde{\gamma}_N$, may not satisfy the first set of constraints in (P3), so we need to find feasible solutions. Towards this end, we let $x' = \frac{\sum_{k=1}^{N}\tilde{x}_k}{N}$, where x denotes α, β and γ. Then we have

$$\begin{aligned}N\alpha' p_m &= \sum_{j=1}^{N}\tilde{\alpha}_j p_m = \sum_{j=1}^{N}\left[\tilde{\beta}_j\mathcal{E}_D\left(\frac{1}{1-\frac{R'}{C}}\right)+\tilde{\gamma}_j p_t\right]\\ &= N\left[\beta'\mathcal{E}_D\left(\frac{1}{1-\frac{R'}{C}}\right)+\gamma' p_t\right].\end{aligned}\tag{35}$$

So we can show that the constraints are also satisfied according to the analysis similar to (30) and (31). In addition, we also have

$$\begin{aligned}&\mathcal{O}_N(\alpha', \beta', \gamma', R', \dots, \alpha', \beta', \gamma', R')\\&\quad= \mathcal{O}_N(\tilde{\alpha}_1, \tilde{\beta}_1, \tilde{\gamma}_1, R', \dots, \tilde{\alpha}_N, \tilde{\beta}_N, \tilde{\gamma}_N, R'). \quad (36)\end{aligned}$$

Noting that $\alpha', \beta', \gamma', R', \dots, \alpha', \beta', \gamma', R'$ also satisfy all the constraints in (P4), we can obtain that

$$\begin{aligned}&\mathcal{O}_N(\alpha', \beta', \gamma', R', \dots, \alpha', \beta', \gamma', R')\\&\quad\le \mathcal{O}_N(\alpha^*, \beta^*, \gamma^*, R^* \dots, \alpha^*, \beta^*, \gamma^*, R^*). \quad (37)\end{aligned}$$

Combining (32), (36) and (37) leads to the fact that $\mathcal{O}_N(\alpha^*, \beta^*, \gamma^*, R^*, \dots, \alpha^*, \beta^*, \gamma^*, R^*) = \mathcal{O}_N(\tilde{\alpha}_1, \tilde{\beta}_1, \tilde{\gamma}_1, \tilde{R}_1, \dots, \tilde{\alpha}_N, \tilde{\beta}_N, \tilde{\gamma}_N, \tilde{R}_N)$.

D. PROOF OF THEOREM 5

There is both energy and data flowing causally between the blocks. Because for a best α, the information forwarded and received must be the same at last, i.e., $\sum_{i=1}^N I_{R_i} = \sum_{i=1}^N I_{T_i}$, we derive that

$$\sum_{i=1}^N \gamma_i = \frac{\sum_{i=1}^N \beta_i R_i}{T(p_t)}. \quad (38)$$

Combining (38) and (15) leads to

$$\begin{aligned}\sum_{i=1}^N (e_i + \alpha_i p_m \tau) &\overset{a}{\ge} \sum_{i=1}^N \left[\beta_i \mathcal{E}_{\mathrm{D}}(\frac{C}{C-R_i})\tau + \frac{\sum_{i=1}^N \beta_i R_i}{T(p_t)} p_t \tau\right]\\&= \sum_{i=1}^N \beta_i \left[\mathcal{E}_{\mathrm{D}}(\frac{C}{C-R_i}) + \frac{R_i}{T(p_t)} p_t\right]\tau, \quad (39)\end{aligned}$$

where (a) is due to the fact that sometimes e_i is too large for the system to use.

We find that $\mathcal{S}(R_i) = \mathcal{E}_{\mathrm{D}}(\frac{C}{C-R_i}) + \frac{R_i}{T(p_t)} p_t$ is an increasing convex function relative to R_i. So we can see $\frac{\sum_{i=1}^N \beta_i \mathcal{S}(R_i)}{\sum_{i=1}^N \beta_i} \ge \mathcal{S}\left(\frac{\sum_{i=1}^N \beta_i R_i}{\sum_{i=1}^N \beta_i}\right)$. We should minimize the right side of (39). So there is an optimum R^* which satisfies

$$R^* = \frac{\sum_{i=1}^N \beta_i R_i}{\sum_{i=1}^N \beta_i}. \quad (40)$$

$\sum_{i=1}^N \beta_i \mathcal{S}(R^*)$ could be seen as the total energy needed during the information transferring. So the optimum $\mathbf{R}$ should be selected as $R^* = \frac{\sum_{i=1}^N \beta_i R_i}{\sum_{i=1}^N \beta_i}$, equal for all the blocks.

E. PROOF OF LEMMA 7

Due to (39) and (18), we have

$$\begin{aligned}&\sum_{i=1}^N \left[e_i + \left(N - (1 + \frac{R}{T(p_t)})\beta_i\right) p_m \tau\right]\\&\quad= \sum_{i=1}^N \left[\beta_i \tau \left(\mathcal{E}_{\mathrm{D}}(\frac{C}{C-R}) + \frac{p_t R}{T(p_t)}\right) + T_i\right]. \quad (41)\end{aligned}$$

so $\sum_{i=1}^N \beta_i = \frac{N p_m \tau + \sum_{i=1}^N e_i - \sum_{i=1}^N T_i}{\left[\mathcal{E}_{\mathrm{D}}(\frac{C}{C-R})\tau + R\frac{p_t}{T(p_t)}\tau + (1+\frac{R}{T(p_t)})p_m \tau\right]}$. We derive the objective function of (P6) as $\mathcal{O}_6 = \sum_{i=1}^N \gamma_i T(p_t)\tau = RT(p_t) \frac{N p_m \tau + \sum_{i=1}^N e_i - \sum_{i=1}^N T_i}{f(R)}$, where $f(R) = (p_t + p_m)R + T(p_t)(p_m + \mathcal{E}_{\mathrm{D}}(\frac{C}{C-R}))$. So according to $\frac{\partial \mathcal{O}_6}{\partial R} = 0$, we have $R\frac{\partial f(R)}{\partial R} - f(R) = 0$, which is equivalent with $\frac{\partial P_1(R)}{\partial R} = 0$.

F. PROOF OF THEOREM 6

Generally, according to the above discussion related to the feasible solution set for (P6) consisting of cases (a)-(d), if there is a feasible solution set $\{W_i, T_i\}$, it could be divided into two parts for all the blocks. One part is the blocks $i \in N_1$ that satisfy $\mathcal{O}_6(W_i, T_i) > 0$ and the other part is the blocks $j \in N_2$ that satisfy $\mathcal{O}_6(W_j, T_j) = 0$. Note that N_2 can be an empty set. As $\sum_{i=1}^N W_i = 0$, we could derive that $\sum_{i=1}^{|N_1|} W_i = -\sum_{j=1}^{|N_2|} W_j$, where $|N_q|$ denotes the number of elements in the set N_q, $q = 1, 2$. Because $\sum_{j=1}^{|N_2|} \mathcal{O}_6(W_j, T_j) = 0$, we have

$$\begin{aligned}&(p_m\tau + \mathcal{E}_{\mathrm{D}}(\frac{C}{C-R^*}))\sum_{j=1}^{|N_2|} W_j\\&\quad= -R^* \sum_{j=1}^{|N_2|} T_j + (p_m \tau + e_i)R^*. \quad (42)\end{aligned}$$

Further we derive that

$$\begin{aligned}&\sum_{i=1}^{|N_1|} \mathcal{O}_6(W_i, T_i)\\&= \sum_{i=1}^{|N_1|} \frac{R^*(p_m\tau + e_i - T_i)}{(p_t + p_m)R^* + T(p_t)(p_m + \mathcal{E}_{\mathrm{D}}(\frac{C}{C-R^*}))}\\&\quad - \sum_{i=1}^{|N_1|} \frac{W_i(p_m + \mathcal{E}_{\mathrm{D}}(\frac{C}{C-R^*}))}{(p_t + p_m)R^*\tau + T(p_t)\tau(p_m + \mathcal{E}_{\mathrm{D}}(\frac{C}{C-R^*}))}\\&\overset{a}{=} \sum_{i=1}^{|N_1|} \frac{R^*(p_m\tau + e_i - T_i)}{(p_t + p_m)R^* + T(p_t)(p_m + \mathcal{E}_{\mathrm{D}}(\frac{C}{C-R^*}))}\\&\quad + \sum_{i=1}^{|N_2|} \frac{W_i(p_m + \mathcal{E}_{\mathrm{D}}(\frac{C}{C-R^*}))}{(p_t + p_m)R^* + T(p_t)(p_m + \mathcal{E}_{\mathrm{D}}(\frac{C}{C-R^*}))}\\&\overset{b}{=} \sum_{i=1}^{|N_1|} \frac{R^*(p_m\tau + e_i - T_i)}{(p_t + p_m)R^* + T(p_t)(p_m + \mathcal{E}_{\mathrm{D}}(\frac{C}{C-R^*}))}\\&\quad + \sum_{j=1}^{|N_2|} \frac{-R^*T_j + (p_m\tau + e_i)R^*}{(p_t + p_m)R^* + T(p_t)(p_m + \mathcal{E}_{\mathrm{D}}(\frac{C}{C-R^*}))}\\&= \sum_{i=1}^{N} \frac{R^*(p_m\tau + e_i) - R^*T_i}{(p_t + p_m)R^* + T(p_t)(p_m + \mathcal{E}_{\mathrm{D}}(\frac{C}{C-R^*}))}\\&= \sum_{i=1}^{|N|} \mathcal{O}_6(0, T_i),\end{aligned}$$

where (a) follows from (P6) and (b) follows from (42).

ACKNOWLEDGMENT

This article was presented in part at the EAI International Conference on Smart Grid and Innovative Frontiers in Telecommunications [1], [2].

REFERENCES

[1] W. Hu, Z. Ni, R. Bhat, Y. Yao, and M. Motani, "Time—Switching energy harvesting relay optimizing considering decoding cost," in *Cloud Computing, Smart Grid and Innovative Frontiers in Telecommunications* (Lecture Notes of the Institute for Computer Sciences, Social Informatics and Telecommunications Engineering), vol. 322, no. 1. Cham, Switzerland: Springer, Dec. 2019, pp. 663–673.

[2] C. Wang, Y. Yao, Z. Ni, R. Bhat, and M. Motani, "Multiple time blocks energy harvesting relay optimizing with time-switching structure and decoding cost," *Cloud Computing, Smart Grid and Innovative Frontiers in Telecommunications* (Lecture Notes of the Institute for Computer Sciences, Social Informatics and Telecommunications Engineering), vol. 322, no. 1. Cham, Switzerland: Springer, Dec. 2020, pp. 615–626.

[3] Z. Yang, W. Xu, Y. Pan, C. Pan, and M. Chen, "Energy efficient resource allocation in machine-to-machine communications with multiple access and energy harvesting for IoT," *IEEE Internet Things J.*, vol. 5, no. 1, pp. 229–245, Feb. 2018.

[4] A. Mehrabi and K. Kim, "Maximizing data collection throughput on a path in energy harvesting sensor networks using a mobile sink," *IEEE Trans. Mobile Comput.*, vol. 15, no. 3, pp. 690–704, Mar. 2016.

[5] S. Tang and L. Tan, "Reward rate maximization and optimal transmission policy of EH device with temporal death in EH-WSNs," *IEEE Trans. Wireless Commun.*, vol. 16, no. 2, pp. 1157–1167, Feb. 2017.

[6] D. K. Verma, R. Y. Chang, and F.-T. Chien, "Energy-assisted decode-and-forward for energy harvesting cooperative cognitive networks," *IEEE Trans. Cognit. Commun. Netw.*, vol. 3, no. 3, pp. 328–342, Sep. 2017.

[7] R. Atallah, M. Khabbaz, and C. Assi, "Energy harvesting in vehicular networks: A contemporary survey," *IEEE Wireless Commun.*, vol. 23, no. 2, pp. 70–77, Apr. 2016.

[8] F. Gholami, H. Meghdadi, and A. Shahzadi, "Throughput analysis for decode- and-forward relaying protocol with wireless energy harvesting and information processing," in *Proc. Int. Conf. Internet Things, Embedded Syst. Commun. (IINTEC)*, Dec. 2018, pp. 132–135.

[9] P. Jindal and R. Sinha, "Energy efficiency and secure communication with power splitting energy harvesting technique for single relay network," in *Proc. Int. Conf. Comput. Appl. (ICCA)*, Sep. 2017, pp. 215–219.

[10] V. M. Blagojevic and A. M. Cvetkovic, "Outage probability of energy harvesting DF relay systems in generalized-K fading," in *Proc. 13th Int. Conf. Adv. Technol., Syst. Services Telecommun. (TELSIKS)*, Oct. 2017, pp. 240–243.

[11] F. Nawaz, S. A. Hassan, and S. Saleem, "Outage analysis of a dual relay SWIPT system in hybrid forwarding schemes," in *Proc. 14th Int. Wireless Commun. Mobile Comput. Conf. (IWCMC)*, Jun. 2018, pp. 1137–1141.

[12] F. Zhang and V. K. N. Lau, "Delay-sensitive dynamic resource control for energy harvesting wireless systems with finite energy storage," *IEEE Commun. Mag.*, vol. 53, no. 8, pp. 106–113, Aug. 2015.

[13] M. K. Sharma and C. R. Murthy, "Packet drop probability analysis of dual energy harvesting links with retransmission," *IEEE J. Sel. Areas Commun.*, vol. 34, no. 12, pp. 3646–3660, Dec. 2016.

[14] H. Liu, K. J. Kim, K. S. Kwak, and H. V. Poor, "QoS-constrained relay control for full-duplex relaying with SWIPT," *IEEE Trans. Wireless Commun.*, vol. 16, no. 5, pp. 2936–2949, May 2017.

[15] X. Huang and N. Ansari, "Optimal cooperative power allocation for energy-harvesting-enabled relay networks," *IEEE Trans. Veh. Technol.*, vol. 65, no. 4, pp. 2424–2434, Apr. 2016.

[16] C. Peng, F. Li, and H. Liu, "Optimal power splitting in two-way decode-and-forward relay networks," *IEEE Commun. Lett.*, vol. 21, no. 9, pp. 2009–2012, Sep. 2017.

[17] A. A. Nasir, X. Zhou, S. Durrani, and R. A. Kennedy, "Throughput and ergodic capacity of wireless energy harvesting based DF relaying network," in *Proc. IEEE Int. Conf. Commun. (ICC)*, Jun. 2014, pp. 1–6.

[18] Y. Ye, Y. Li, D. Wang, F. Zhou, R. Q. Hu, and H. Zhang, "Optimal transmission schemes for DF relaying networks using SWIPT," *IEEE Trans. Veh. Technol.*, vol. 67, no. 8, pp. 7062–7072, Aug. 2018.

[19] V. M. Blagojević, A. M. Cvetković, and P. N. Ivaniš, "Performance analysis of energy harvesting DF relay system in generalized-K fading environment," *Phys. Commun.*, vol. 28, pp. 190–200, Jun. 2018.

[20] M. Abedi, H. Masoumi, and M. J. Emadi, "Power splitting-based SWIPT systems with decoding cost," *IEEE Wireless Commun. Lett.*, vol. 8, no. 2, pp. 432–435, Apr. 2019.

[21] K. Tutuncuoglu, B. Varan, and A. Yener, "Throughput maximization for two-way relay channels with energy harvesting nodes: The impact of relaying strategies," *IEEE Trans. Commun.*, vol. 63, no. 6, pp. 2081–2093, Jun. 2015.

[22] L. Shi, Y. Ye, R. Q. Hu, and H. Zhang, "System outage performance for three-step two-way energy harvesting DF relaying," *IEEE Trans. Veh. Technol.*, vol. 68, no. 4, pp. 3600–3612, Apr. 2019.

[23] M. C. Ju and H.-C. Yang, "Optimum design of energy harvesting relay for two-way decode- and-forward relay networks under max–min and max-sum criterions," *IEEE Trans. Commun.*, vol. 67, no. 10, pp. 6682–6697, Oct. 2019.

[24] N. T. P. Van, S. F. Hasan, X. Gui, S. Mukhopadhyay, and H. Tran, "Three-step two-way decode and forward relay with energy harvesting," *IEEE Commun. Lett.*, vol. 21, no. 4, pp. 857–860, Apr. 2017.

[25] Y. S. Rao, R. P. Sirigina, and A. S. Madhukumar, "On the DMT of RF energy harvesting-based dynamic decode- and-forward relaying," *IEEE Commun. Lett.*, vol. 21, no. 1, pp. 200–203, Jan. 2017.

[26] Y. Zou, J. Zhu, and X. Jiang, "Joint power splitting and relay selection in energy-harvesting communications for IoT networks," *IEEE Internet Things J.*, vol. 7, no. 1, pp. 584–597, Jan. 2020.

[27] K. Reshma and A. V. Babu, "Throughput analysis of energy harvesting enabled incremental relaying NOMA system," *IEEE Commun. Lett.*, vol. 24, no. 7, pp. 1419–1423, Jul. 2020.

[28] X. Lan, Y. Zhang, Q. Chen, and L. Cai, "Energy efficient buffer-aided transmission scheme in wireless powered cooperative NOMA relay network," *IEEE Trans. Commun.*, vol. 68, no. 3, pp. 1432–1447, Mar. 2020.

[29] C. Guo, J. Xin, L. Zhao, and X. Chu, "Performance analysis of cooperative NOMA with energy harvesting in multi-cell networks," *China Commun.*, vol. 16, no. 11, pp. 120–129, Nov. 2019.

[30] C. Zhang, H. Du, and J. Ge, "Energy-efficient power allocation in energy harvesting two-way AF relay systems," *IEEE Access*, vol. 5, pp. 3640–3645, 2017.

[31] M. Zhao, J. Zhao, W. Zhou, J. Zhu, and S. Zhang, "Energy efficiency optimization in relay-assisted networks with energy harvesting relay constraints," *China Commun.*, vol. 12, no. 2, pp. 84–94, Feb. 2015.

[32] A. Rauniyar, P. E. Engelstad, and O. N. Osterbo, "Performance analysis of RF energy harvesting and information transmission based on NOMA with interfering signal for IoT relay systems," *IEEE Sensors J.*, vol. 19, no. 17, pp. 7668–7682, Sep. 2019.

[33] Z. Ni, R. V. Bhat, and M. Motani, "On dual-path energy-harvesting receivers for IoT with batteries having internal resistance," *IEEE Internet Things J.*, vol. 5, no. 4, pp. 2741–2752, Aug. 2018.

[34] P. Grover, K. Woyach, and A. Sahai, "Towards a communication-theoretic understanding of system-level power consumption," *IEEE J. Sel. Areas Commun.*, vol. 29, no. 8, pp. 1744–1755, Sep. 2011.

[35] Z. Ni and M. Motani, "Performance of energy-harvesting receivers with time-switching architecture," *IEEE Trans. Wireless Commun.*, vol. 16, no. 11, pp. 7252–7263, Nov. 2017.

[36] Z. Ni and M. Motani, "Performance of energy harvesting receivers with power optimization," *IEEE Trans. Commun.*, vol. 66, no. 3, pp. 1309–1321, Mar. 2018.

[37] A. Arafa and S. Ulukus, "Optimal policies for wireless networks with energy harvesting transmitters and receivers: Effects of decoding costs," *IEEE J. Sel. Areas Commun.*, vol. 33, no. 12, pp. 2611–2625, Dec. 2015.

[38] K. Tutuncuoglu and A. Yener, "Communicating with energy harvesting transmitters and receivers," in *Proc. Inf. Theory Appl. Workshop*, Feb. 2012, pp. 240–245.

[39] H. Mahdavi-Doost and R. D. Yates, "Energy harvesting receivers: Finite battery capacity," in *Proc. IEEE Int. Symp. Inf. Theory*, Jul. 2013, pp. 1799–1803.

[40] R. D. Yates and H. Mahdavi-Doost, "Energy harvesting receivers: Optimal sampling and decoding policies," in *Proc. IEEE Global Conf. Signal Inf. Process.*, Dec. 2013, pp. 367–370.

[41] H. Mahdavi-Doost and R. D. Yates, "Fading channels in energy-harvesting receivers," in *Proc. 48th Annu. Conf. Inf. Sci. Syst. (CISS)*, Mar. 2014, pp. 367–370.

[42] R. Nagda, S. Satpathi, and R. Vaze, "Optimal offline and competitive online strategies for transmitter-receiver energy harvesting," in *Proc. IEEE Int. Conf. Commun. (ICC)*, Jun. 2015, pp. 74–79.

[43] A. Arafa, A. Baknina, and S. Ulukus, "Energy harvesting two-way channels with decoding and processing costs," *IEEE Trans. Green Commun. Netw.*, vol. 1, no. 1, pp. 3–16, Mar. 2017.

[44] O. Ozel, K. Tutuncuoglu, J. Yang, S. Ulukus, and A. Yener, "Transmission with energy harvesting nodes in fading wireless channels: Optimal policies," *IEEE J. Sel. Areas Commun.*, vol. 29, no. 8, pp. 1732–1743, Sep. 2011.

[45] N. Zhao, F. Hu, Z. Li, and Y. Gao, "Simultaneous wireless information and power transfer strategies in relaying network with direct link to maximize throughput," *IEEE Trans. Veh. Technol.*, vol. 67, no. 9, pp. 8514–8524, Sep. 2018.
[46] L. Shi, W. Cheng, Y. Ye, H. Zhang, and R. Q. Hu, "Heterogeneous power-splitting based two-way DF relaying with non-linear energy harvesting," in *Proc. IEEE Global Commun. Conf. (GLOBECOM)*, Dec. 2018, pp. 1–7.
[47] D. Zhao, H. Zhao, M. Jia, and W. Xiang, "Smart relaying for selection combining based decode- and-forward cooperative networks," *IEEE Commun. Lett.*, vol. 18, no. 1, pp. 74–77, Jan. 2014.
[48] G. Wang, W. Xiang, and J. Yuan, "Generalized wireless network coding schemes for multihop two-way relay channels," *IEEE Trans. Wireless Commun.*, vol. 13, no. 9, pp. 5132–5147, Sep. 2014.
[49] F. Zhang and V. K. N. Lau, "Closed-form delay-optimal power control for energy harvesting wireless system with finite energy storage," *IEEE Trans. Signal Process.*, vol. 62, no. 21, pp. 5706–5715, Nov. 2014.
[50] S. L. Pong, V. Y. F. Tan, and A. Ozgur, "On achievable rates of AWGN energy-harvesting channels with block energy arrival and non-vanishing error probabilities," in *Proc. IEEE Int. Symp. Inf. Theory (ISIT)*, Jun. 2017, pp. 814–818.
[51] D. Shaviv and A. Oezguer, "Online power control for block i.i.d. energy harvesting channels," in *Proc. IEEE Global Commun. Conf. (GLOBECOM)*, Dec. 2017, pp. 1–6.
[52] R. V. Bhat, M. Motani, and T. J. Lim, "Energy harvesting communications without transmitter channel state information using layered coding," *IEEE Trans. Green Commun. Netw.*, vol. 2, no. 1, pp. 127–142, Mar. 2018.
[53] P. Lee, Z. A. Eu, M. Han, and H.-P. Tan, "Empirical modeling of a solar-powered energy harvesting wireless sensor node for time-slotted operation," in *Proc. IEEE Wireless Commun. Netw. Conf.*, Mar. 2011, pp. 179–184.
[54] T.-Q. Wu and H.-C. Yang, "On the performance of overlaid wireless sensor transmission with RF energy harvesting," *IEEE J. Sel. Areas Commun.*, vol. 33, no. 8, pp. 1693–1705, Aug. 2015.
[55] Z. Zhou, M. Peng, Z. Zhao, W. Wang, and R. S. Blum, "Wireless-powered cooperative communications: Power-splitting relaying with energy accumulation," *IEEE J. Sel. Areas Commun.*, vol. 34, no. 4, pp. 969–982, Apr. 2016.
[56] G. Huang and W. Tu, "On opportunistic energy harvesting and information relaying in wireless-powered communication networks," *IEEE Access*, vol. 6, pp. 55220–55233, 2018.
[57] X. Di, K. Xiong, P. Fan, and H.-C. Yang, "Simultaneous wireless information and power transfer in cooperative relay networks with rateless codes," *IEEE Trans. Veh. Technol.*, vol. 66, no. 4, pp. 2981–2996, Apr. 2017.
[58] G. Huang and W. Tu, "A high-throughput wireless-powered relay network with joint time and power allocations," *Comput. Netw.*, vol. 160, pp. 65–76, Sep. 2019.
[59] S. Boyd and L. Vandenberghe, *Convex Optimization*. Cambridge, U.K.: Cambridge Univ. Press, 2004.

YANXIN YAO (Member, IEEE) received the B.E. degree in communication engineering from Jilin University, in 2005, and the Ph.D. degree in communication and information systems from Beihang University, China, in 2010. She is currently a Professor with Beijing Information Science & Technology University. She held a postdoctoral position with Beihang University and was a Visiting Fellow with the National University of Singapore. Her current research interests include intelligent signal processing and network optimization. She was awarded as the Excellent Talent by Beijing Organization Department and the Top Talent by Beijing Municipal Education Commission. She has hosted many projects, including the National Natural Science Foundation of China and the Natural Science Foundation of Beijing.

ZHENGWEI NI (Member, IEEE) received the B.E. and M.E. degrees from the Beijing University of Posts and Telecommunications, Beijing, China, and the Ph.D. degree from the National University of Singapore. He is currently a Lecturer with Zhejiang Gongshang University, Hangzhou, China. He has published several articles on energy harvesting optimization.

WANQIU HU received the B.E. degree from the Hebei University of Technology, in 2018. She is currently pursuing the master's degree with Beijing Information Science & Technology University. Her current research interest includes intelligent signal processing.

MEHUL MOTANI (Fellow, IEEE) received the B.E. degree from The Cooper Union, New York, NY, USA, the M.S. degree from Syracuse University, Syracuse, NY, and the Ph.D. degree from Cornell University, Ithaca, NY, all in electrical and computer engineering. He was a Research Scientist with the Institute for Infocomm Research, Singapore, for three years, and a Systems Engineer at Lockheed Martin, Syracuse, for over four years. He is currently an Associate Professor with the Department of Electrical and Computer Engineering, National University of Singapore (NUS), and a Visiting Research Collaborator with Princeton University, where he was a Visiting Fellow. His research interests include information theory and coding theory, machine learning, biomedical informatics, wireless and sensor networks, and the Internet of Things. He was a recipient of the Intel Foundation Fellowship for his Ph.D. research, the NUS Annual Teaching Excellence Award, the NUS Faculty of Engineering Innovative Teaching Award, and the NUS Faculty of Engineering Teaching Honours List Award. He actively participates in the Institute of Electrical and Electronics Engineers (IEEE) and the Association for Computing Machinery (ACM). He has served as the Secretary for the IEEE Information Theory Society Board of Governors. He has served as an Associate Editor for the IEEE TRANSACTIONS ON INFORMATION THEORY and the IEEE TRANSACTIONS ON COMMUNICATIONS. He has also served on the organizing and technical program committees of numerous IEEE and ACM conferences.